

REPORT DOCUMENTATION PAGE

Form Approved
OMB No. 0704-0188

Public reporting burden for this collection of information is estimated to average 1 hour per response, including the time for reviewing instructions, searching existing data sources, gathering and maintaining the data needed, and completing and reviewing this collection of information. Send comments regarding this burden estimate or any other aspect of this collection of information, including suggestions for reducing this burden to Department of Defense, Washington Headquarters Services, Directorate for Information Operations and Reports (0704-0188), 1215 Jefferson Davis Highway, Suite 1204, Arlington, VA 22202-4302. Respondents should be aware that notwithstanding any other provision of law, no person shall be subject to any penalty for failing to comply with a collection of information if it does not display a currently valid OMB control number. **PLEASE DO NOT RETURN YOUR FORM TO THE ABOVE ADDRESS.**

1. REPORT DATE UNCLASSIFIED			2. REPORT TYPE Annual			3. DATES COVERED UNCLASSIFIED		
4. TITLE AND SUBTITLE Peripheral Nerve Repair and Prevention of Neuroma Formation						5a. CONTRACT NUMBER		
						5b. GRANT NUMBER W81XWH-13-1-0286		
						5c. PROGRAM ELEMENT NUMBER		
6. AUTHOR(S) Alan R. Davis, Ph.D. E-Mail:ardavis@bcm.edu						5d. PROJECT NUMBER		
						5e. TASK NUMBER		
						5f. WORK UNIT NUMBER		
7. PERFORMING ORGANIZATION NAME(S) AND ADDRESS(ES) Baylor College of Medicine Houston TX 77030						8. PERFORMING ORGANIZATION REPORT NUMBER		
9. SPONSORING / MONITORING AGENCY NAME(S) AND ADDRESS(ES) U.S. Army Medical Research and Materiel Command Fort Detrick, Maryland 21702-5012						10. SPONSOR/MONITOR'S ACRONYM(S)		
						11. SPONSOR/MONITOR'S REPORT NUMBER(S)		
12. DISTRIBUTION / AVAILABILITY STATEMENT Approved for Public Release; Distribution Unlimited								
13. SUPPLEMENTARY NOTES								
14. ABSTRACT An overarching hypothesis of this application is that the ADRB3 ⁺ perineurial progenitor cells functionally contribute to both nerve and bone regeneration and during amputation these processes are aberrant leading to neuroma formation and HO. We proposed that neuroma formation could potentially be suppressed through selective modulation of neural inflammation. We have previously shown that inhibition of selective targets in this cascade can inhibit heterotopic ossification (HO). We established a model of neuroma in rats and found that delivery of cromolyn, suppressed the size of the neuromas. We proposed that cromolyn, which blocks mast cell degranulation, serotonin release, leads to the suppression of the ADRB3 ⁺ perineurial cells, and ultimately reduction or ablation of neuroma. The tissues are further being analyzed to confirm the molecular pathway has been altered as predicted. We are working on a system to measure the volume of the neuroma for comparison in these studies. Finally we have received several peripheral nerves from humans, and have been isolating the ADRB3 ⁺ cells, for characterization of selective markers as well as for culturing experiments in the rat. These are ongoing experiments. We have also received some human tissues from HO and have been analyzing the environment identified in these biopsies including the nerve structure which is present in the biopsy samples.								
15. SUBJECT TERMS Neuroma, bone morphogenetic protein 2, perineurial progenitors, brown adipose, heterotopic ossification.								
16. SECURITY CLASSIFICATION OF:				17. LIMITATION OF ABSTRACT	18. NUMBER OF PAGES	19a. NAME OF RESPONSIBLE PERSON		
a. REPORT	b. ABSTRACT	c. THIS PAGE	USAMRMC					
Unclassified	Unclassified	Unclassified	Unclassified		46	19b. TELEPHONE NUMBER (include area code)		

Table of Contents

	<u>Page</u>
1. Introduction.....	4
2. Keywords.....	4
3. Accomplishments.....	4-19
4. Impact.....	19-20
5. Changes/Problems.....	21
6. Products.....	21
7. Participants & Other Collaborating Organizations.....	21
8. Special Reporting Requirements.....	21
9. Appendices.....	21-46

INTRODUCTION: We have recently isolated and initially characterized a unique stem-progenitor in the perineurium of adult peripheral nerves that has properties similar to a CNS glial cell. We have identified key cytokines-growth factors that cause these cells to replicate and have shown *in vivo* that they can migrate from the peripheral nerve during times of injury or growth to function in patterning axonal growth. We have recently shown that these cells express the neural guidance molecule reelin, which in the CNS functions to pattern axonal growth. Additionally, our data indicates that these cells also traffic triglyceride for energy and provide lipids for myelination of the extending nerve. Interestingly, these cells play a critical role in heterotopic bone formation. Thus, new bone formation appears to be closely linked to nerve remodeling and growth. The data suggests that there is a common basic mechanism that is shared between neuroma formation and heterotopic ossification (HO) in severe trauma and amputation, suggesting that both may be aberrant attempts to regenerate missing tissues. We propose to (1) isolate the human counterpart of the mouse transient brown adipocyte, and (2) demonstrate in athymic rats that these cells function similarly to the mouse counterpart. Additionally, we will utilize a population of these cells already isolated from dog, and continue to develop them in a canine model of peripheral nerve extension- repair as well as characterize their contribution to bone fracture repair. Finally, (3) we will suppress the formation of HO and neuromas (known to occur in the residual limb after amputation in humans) through selective targeting of the initial cytokines-growth factors, that drive the activation, replication, egress of perineurial progenitors from the peripheral nerve, and their ultimate differentiation. These studies, using both the human counterpart as well as a large animal model, will provide additional data beyond our current small animal studies that will allow us to rapidly translate this into the clinic. Although there is significant work to develop these cells for clinical use, this application will provide proof of principal and initial efficacy data to warrant future investigation where they could then be combined with current nerve conduits and/or current strategies for bone repair.

KEYWORDS: Neuroma, bone morphogenetic protein 2, perineurial progenitors, brown adipose, heterotopic ossification.

ACCOMPLISHMENTS:

What were the major goals of the project?

Task 1: To test the functional contribution of the mouse/human cells (athymic rats) and their canine counterpart (canine) in critical size nerve and bone tissue repair.

- *Subaim 1: Demonstration of functional contribution of the perineurial progenitor cells to nerve repair.*

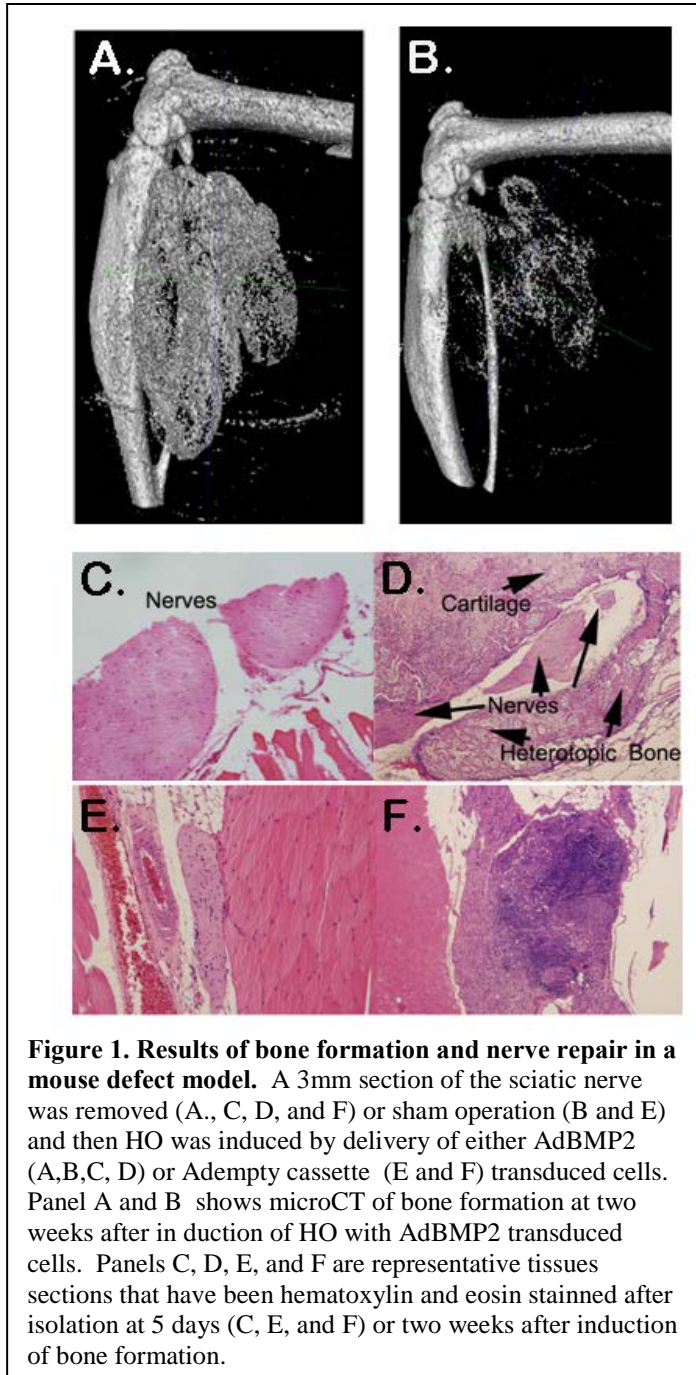
i. Secure ACURO approval for the animal studies - Completed

ii. Testing mouse cells in an athymic rat defect model.

- i. Athymic rats will undergo nerve resection to introduce defects (1 and 5 mm) into the sciatic nerve. Perineurial cells (10^6) (mouse-C57BL/6-green fluorescent protein (GFP) or human above) will delivered at the time of nerve defects. (Months 3-15 (mouse) 15-36 human)*

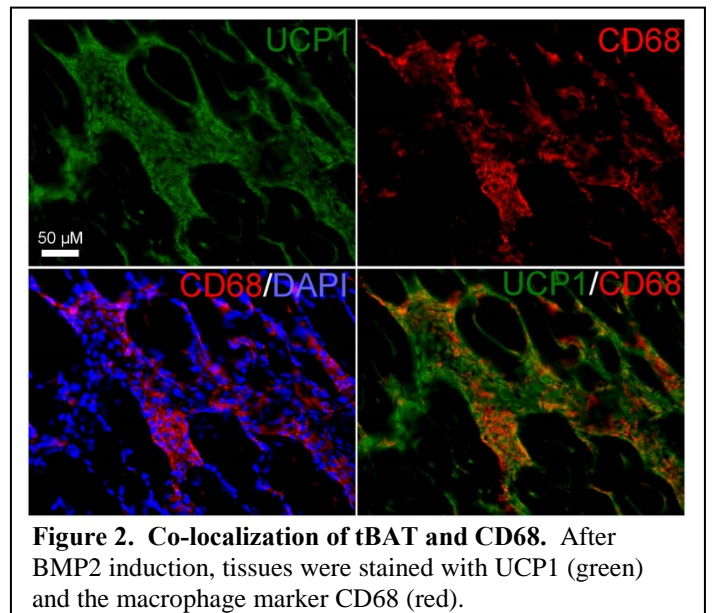
This model has been established and we have initiated experiments. Our first experiments were to introduce a small defect (5 mm) into the nerve, and then to induce heterotopic ossification by delivery of AdBMP2 or Adempty cassette transduced cells. This initial experiment was performed because this would demonstrate whether expansion and recruitment of the perineurial progenitors led to repair of the defect. In these experiments a 5 mm section of the sciatic nerve was removed or a control sham operation was performed. One week later AdBMP2 or Adempty transduced cells were injected into the hindlimb. Nerve repair was characterized at 5 days after these injections or 12 days after the initial nerve injury. Briefly the tissues were isolated, the long bones removed and then snap frozen. Tissues were then serially sectioned to generate 30 slides. Then every 5th slide was hematoxylin and eosin stained and the reaction area was located. In many cases there was no reaction area and therefore another 30 sections would be cut. The tissue was then systematically sectioned as described until the entire region of interest has been located on the slides. Then these slides were further subject to immunostaining for the markers below. Representative photomicrographs of the hematoxylin and eosin stained tissues are shown in Figure 1 (panels C, E, and F). The animals receiving AdBMP2 transduced cells (Fig 1, panel C and D) appeared to have normal nerves. In no cases could we locate the defect in the nerve that had been introduced through scanning over 200 sections from day 5 tissues (n=3). Further, the resultant heterotopic ossification in the animals that had a 5 mm section removed was wrapped around the nerve, encompassing it, but keeping it intact (Figure 1, panel D). Bone formation surrounding peripheral nerves is similar to that observed in military scenarios of heterotopic ossification that occur after amputation. Further there appeared to be more bone formation in the animals receiving the defect as compared to the sham operated animals, suggesting that the nerve transection may enhance heterotopic ossification. Again the findings are

similar to the findings in military populations. What was extremely surprising to us was the resultant nerves in animals receiving the control Adempty cassette transduced cells. Animals receiving sham surgery, had normal nerves, and the transduced cells were no longer present in the muscle as expected from previous studies (1).



However, the animals, which had received the 5 mm nerve defect not only did not heal, but the presence of the AdEmpty transduced cells appeared to lead to what appears to be a neuroma-like structure (Figure 1, panel F). However these cells are more macrophage in appearance, than those observed in our other models of neuroma, suggesting that the addition of foreign materials to the site is affecting the nerve healing. Interestingly, recent studies in the mouse focused on further characterizing these perineurial cells suggests that a subpopulation of these cells may possess several macrophage markers and may represent the differentiation of the perineurial progenitors to the macrophage phenotype leading to neuroma formation (Figure 2).

We are currently further analyzing these tissues and repeating these experiments. Additionally, we have set up ongoing experiments to repeat these studies, but adding perineurial cells as an additional variable. In these studies, animals will either have sham or 5 mm nerve resection of the nerve and then receive AdBMP2 or Adempty transduced cells with and without the



mouse perineurial cells isolated from C57BL6-GFP mice. All tissues will be analyzed for the markers (GFP, protein gene product – (PGP9.5), proteolipid protein (PLP), S100B, occludin, neurofilament, glial cell-derived neurotrophic factor (GDNF), brain-derived neurotrophic factor (BDNF), uncoupling protein 1 (UCP1, and reelin). However, we will select an additional earlier time point (3 days) in these experiments to since the reaction-healing appears to be very rapid. The nerves will also be tested for electrical conductance. We propose that these experiments will be completed for publication in the next 6 months.

As for the human perineurial cells, we will attempt to also start these in the next couple of months. We have been working on feasibility of the nerve harvest and maintenance of the cells. As described in aim 3, the cells and nerve tissues have been fixed, due to timing of when they can be sorted by FACS. We propose to move to a magnetic separation method to isolate the ADR β 3⁺ cells, which may not be as pure as a FACS isolated population, but allow for a much shorter preparation time, prior to injection into the animals.

ii *Testing canine perineurial cells in a canine nerve defect model.* 0.5-2.0 cm defects will be introduced into the dog sciatic nerve. Perineurial progenitors will be injected with and without an additional commercial conduit (Axoguard Nerve Connector, AxoGen Inc) (**Months 15-36**)

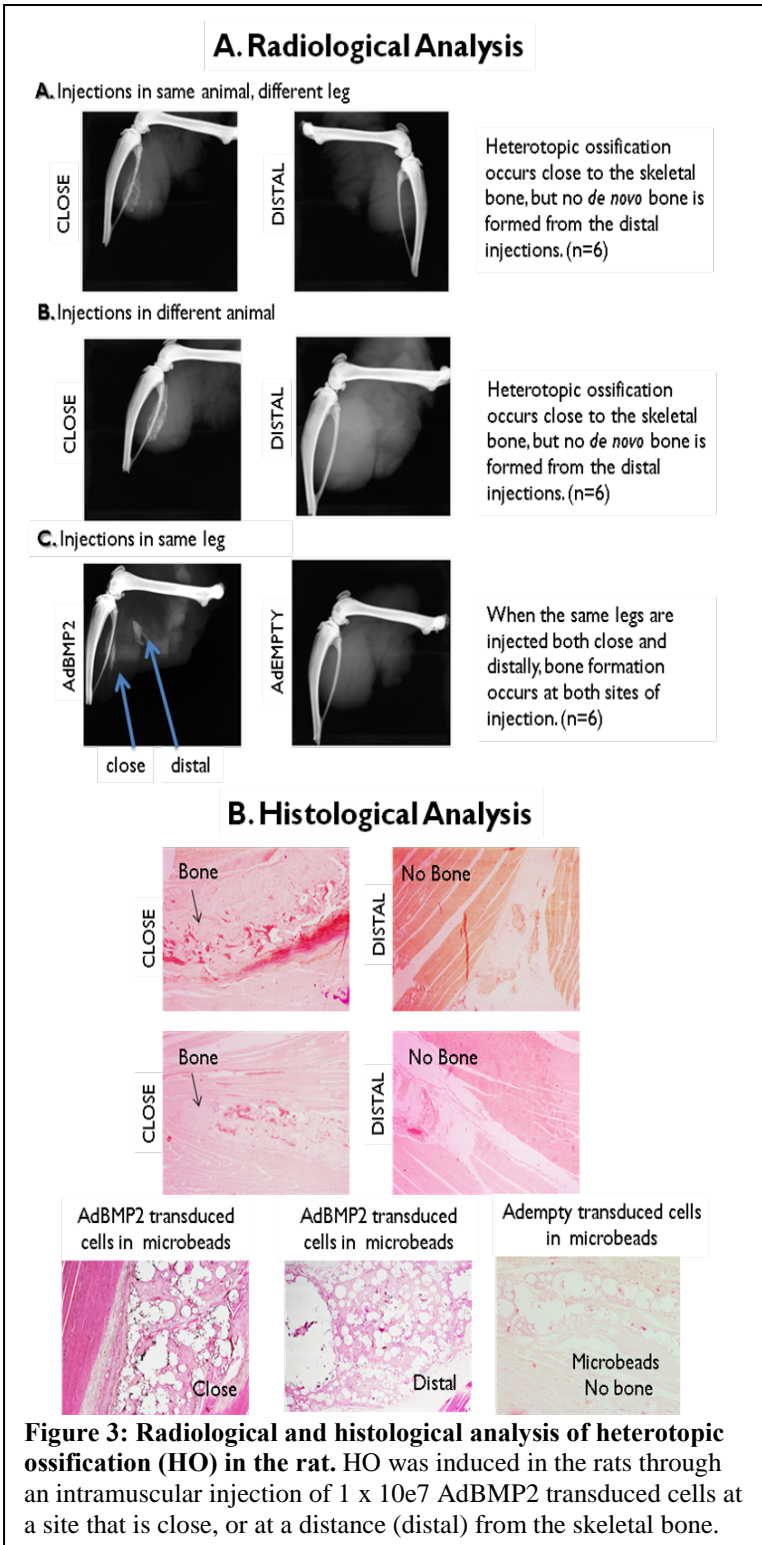
- a. After 10 days, nerves will be isolated and subject to TEM (transmission electron microscopy) to determine the degree of myelination
- b. Electrical conductance measurements

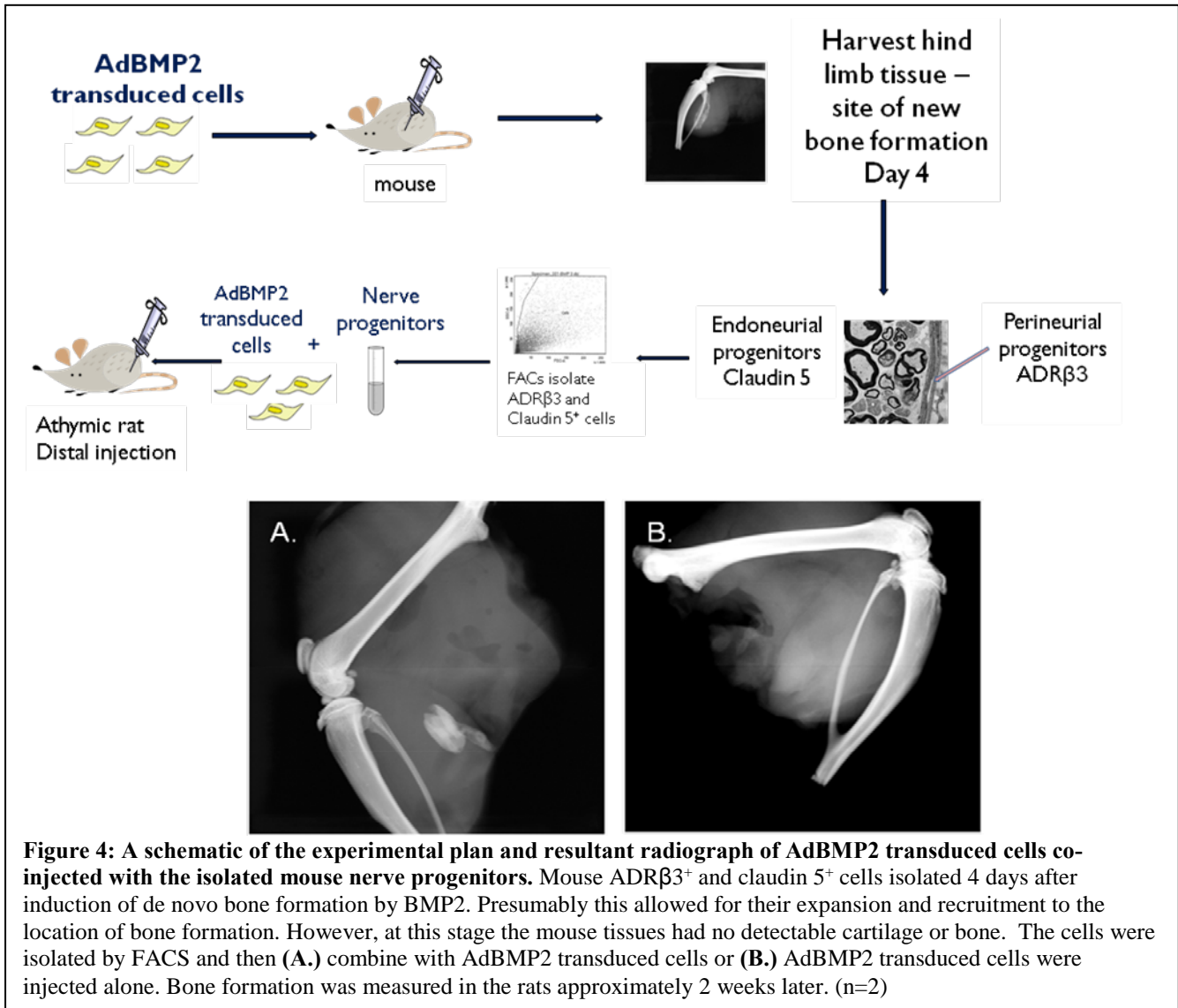
We will most likely start these experiments in the next 4-6 months, as we complete the rat experiments.

- *Subaim 2: Demonstration of functional contribution of the perineurial cells to bone repair:*

- i. *Testing in a rat HO model*

We will first tested the ability of the $ADR\beta3^+$ perineurial progenitors to rescue heterotopic ossification in a rat model. We recently found that heterotopic ossification was unable to form if the injection of BMP2-producing cells was too far from the skeletal long bone (Figure 3). When the AdBMP2 cells were placed near the skeletal bone, the reaction would progress even though there was no fusion as determined by histology. Alternatively, when injection was placed at a distance from the bone then heterotopic ossification did not occur. We next attempted to bone formation at the more distant sight by inclusion of the perineurial progenitors. However, we were again unable to observe bone formation at a distal location. Therefore we next isolated the claudin 5⁺ population by cell sorting from C57BL/6GFP mouse tissues 4 days after receiving the AdBMP2 transduced cells. We also simultaneously isolated the $ADR\beta3^+$ perineurial progenitors (this is the UCP1⁺ population Salisbury *et al*, 2012), which is the other cell population in mice that is derived from peripheral nerves 4 days after induction of *de novo* bone formation. These two populations of nerve derived progenitors were pooled and 1 million cells were co-injected with the AdBMP2 transduced cells at the distal location in the rat hind limb. The radiographic analysis suggested that these progenitors could rescue the bone formation (Figure 4).





ii. Testing in a canine bone defect model: We will introduce a 3 cm critical size defect into the canine femur and the bone ends/defect size is fixed using an internal bone plate. **(Months 6- 18)**

Our preliminary data obtained using other funding sources, suggested that delivery of the AdBMP2-transduced cells to the canine femur model did not result in bone formation and healing. In this aim we proposed to look at whether delivery of the ADR β 3 cells along with the AdBMP2-transduced cells would enhance bone repair. However, the studies in the rat heterotopic ossification model described above (Figure 3), suggest that low dose sustained BMP2-induced bone formation was not rescued until two peripheral nerve stem cells were provided. In these experiments the perineurial cells used to rescue bone formation were already expanding, presumably due to the activation of the sympathetic nervous system by noradrenaline (2). Therefore we have been focused on translating this to the dog model; however, we are not sure that we can activate canine ADR β 3+ cells. We have therefore isolated the sciatic nerve from a previous dog experiment and we propose to culture them briefly in noradrenaline and BMP2 to induce bone formation. These studies will be initiated only when we have optimized this using the rat model. At that point we will move to the dog, and thus these have been delayed from our estimated start date. We propose that these will start in 4-6 months.

- a. *Histological analysis:* Bone formation will be assessed by histological analysis of three samples
- b. *Radiological analysis:* X-rays will be taken starting at two weeks after surgery. Dogs will be maintained and x-rayed every two weeks, until 6 weeks. If no obvious bone by x-ray has formed the dogs will be euthanized. If we observe bone formation, then bone healing will be allowed to proceed for another 2-4 months. Upon euthanasia the bone will be subject to computational tomography (CT) analysis using a clinical grade CT at University of Texas Medical Branch (UTMB). The tissues will then be submitted for both biomechanical analysis and histological analysis. To reduce animal number we will perform all three techniques on the same tissues. In the absence of bone formation no biomechanical analysis will be performed.
- c. *Biomechanical analysis:* Torsional testing will be performed on femurs after healing by torsional testing using equipment in Dr. Zbigniew Gugala's laboratory. For all torsional biomechanical testing of bone healing, the contralateral femur will serve as the control. The failure torque of the treated femur will be normalized to the failure torque of the contra-lateral control.

Task 2: To suppress neuroma and heterotopic ossification after amputation, we will selectively target specific cytokines/growth factors in the neuroinflammatory cascade to stop the process that drives the activation, replication, egress from the peripheral nerve, and ultimate differentiation of these perineurial cells.

i. Neuroma formation in rats with a constricted sciatic nerve and pre-treatment with drug: (Months 3-24)

We initiated studies to induce the neuromas in the Wistar rat model. In these studies we set up the neuroma model as described in our animal protocol by loosely ligating the sciatic nerve using chromic gut sutures. The control is a sham operation in which the nerve is exposed, but the chromic gut is not placed on the nerve. In no cases did the sham group result in neuroma formation. However, as seen in Figure 5, we were able to routinely obtain neuromas in the sciatic nerve using this procedure.

We then initiated experiments to determine if rats (n=6) receiving vehicle (saline) or drug (sodium cromoglycate 150 mg/kg intraperitoneal route) would suppress the neuroma formation. Results showed the presence of neuromas in both cromolyn treated and untreated groups, however the neuromas in the cromolyn treated are actually appear to be significantly smaller. In these experiments, we took measurements, but did not want to disrupt the neuroma in order to be able to carefully analyze the tissues histologically to determine what

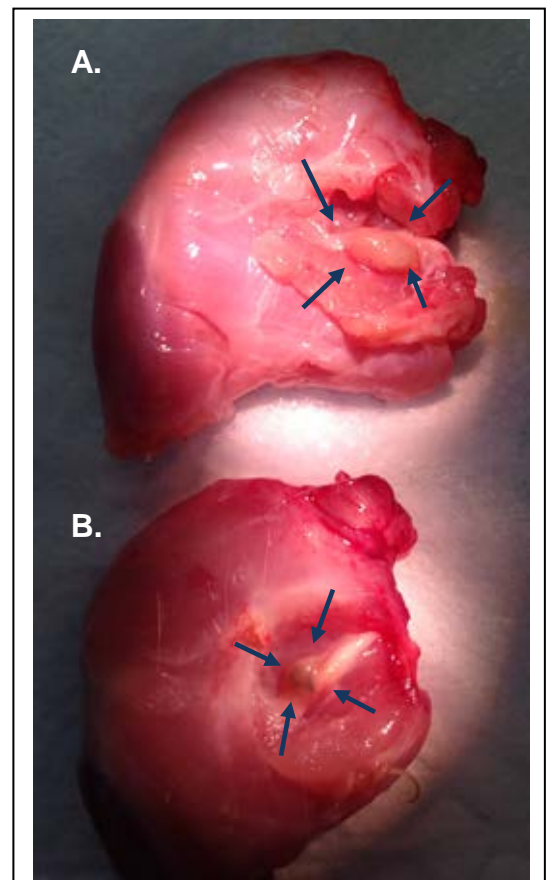
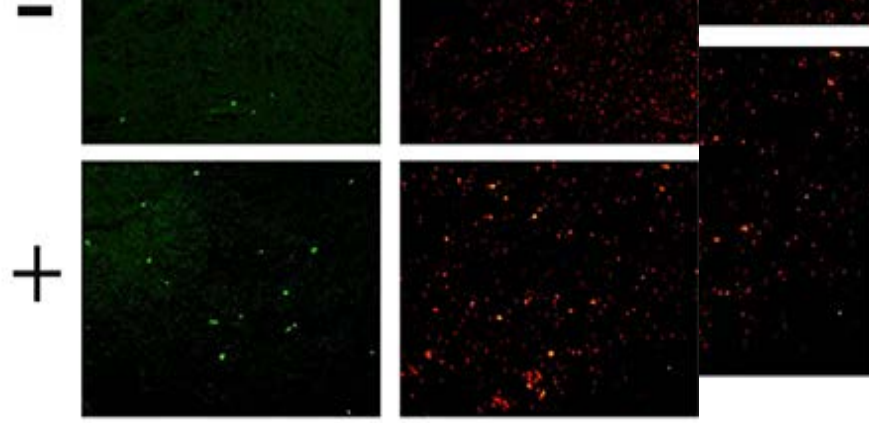


Figure 5: Photo of resultant neuromas in Wistar Rats. Neuromas were introduced by making two constrictures in the sciatic nerve with surgical sutures in the (A.) absence and (B.) presence of cromolyn. Arrows show the location of the neuroma within the rat sciatic nerve.



tissue was not harvested from the muscle, embedded and serially sectioned generated for the presence of claudin 5 positive cells in the muscle. However, although staining in the muscle, consistent with previous results, it appears likely that cromolyn blocks the formation of all other downstream events. It also blocks the formation of all other downstream events. It also blocks the formation of all other downstream events.

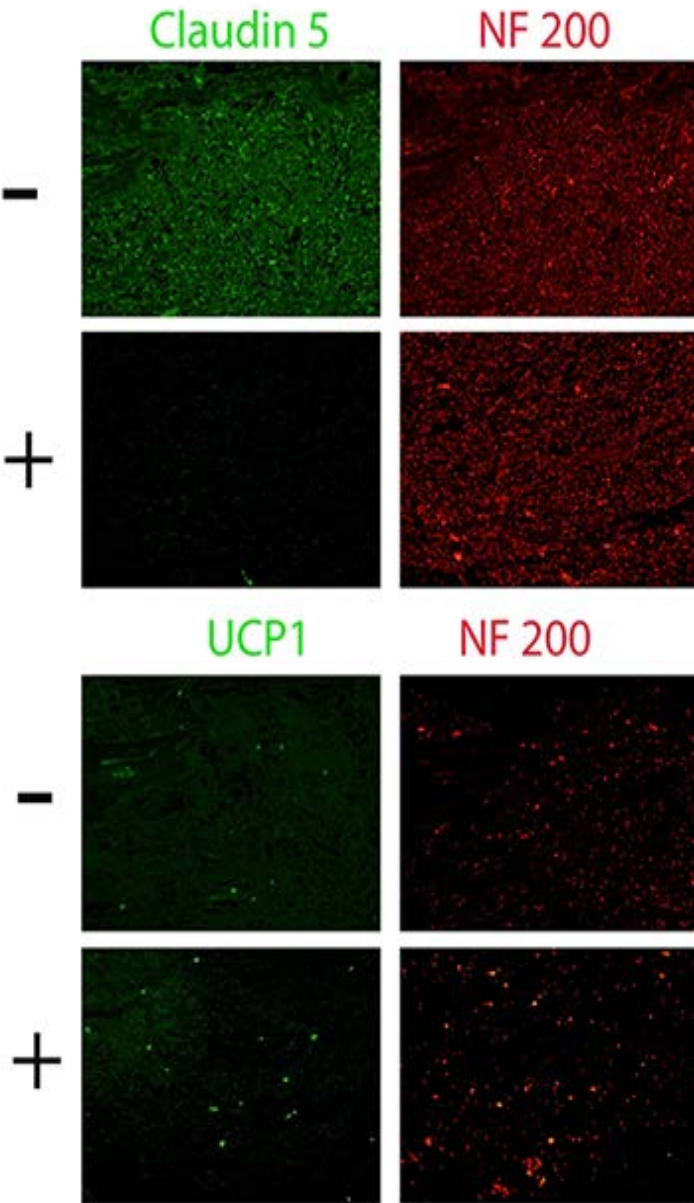
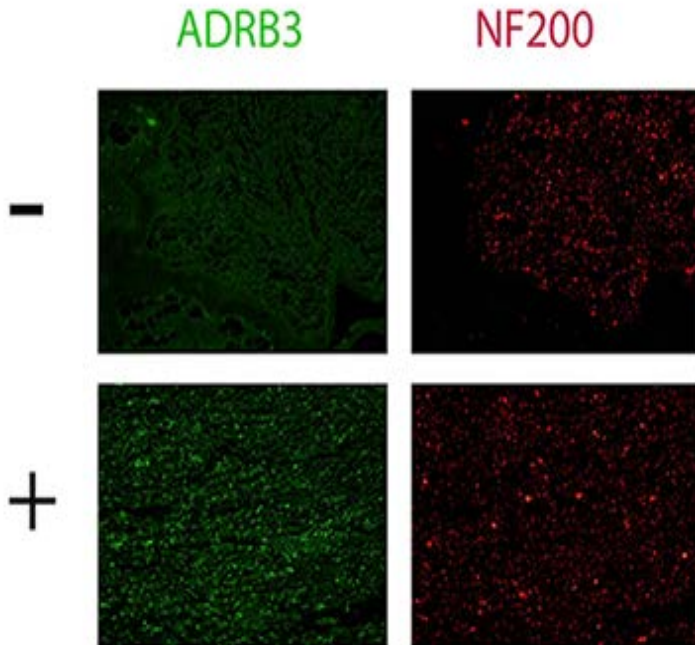


Figure 6 Inhibition of neuroma formation by cromolyn. Neuroma formation was initiated with chronic gut as described above either in the presence (+) or absence (-) of sodium cromolyn. After 2 weeks mice (n=6 per group) were euthanized and frozen sections prepared around the site of application of the chronic gut. These sections were stained for either claudin 5, UCP1, or ADRB3 (all green) in combination with NF 200 (red).



We are also currently repeating this with cromolyn that is tested in mouse simultaneously to ensure that it is suppressing heterotopic ossification in this model as we have previously demonstrated (3). The bioavailability of cromolyn is poor because of poor solubility. We will therefore confirm that the suppression of the neuroma is the result of active drug by simultaneous testing of the effect of the same lot of cromolyn on HO. We also plan in the next project period two other compounds. Newborn rats have been treated with capsaicin, and we are currently allowing them to mature for these experiments. Additionally we will start the ADR β 3 antagonist studies in the next 6 months. We are also continuing to develop a system to demonstrate statistically that the drugs have suppressed the neuroma. To this end, we will isolate the neuromas from the vehicle treated as well as the drug treated and both measure and weigh them. This will allow us to quantify the differences and support the qualitative histological evaluation of the additional subset of samples. Finally, to quantitate the histological evaluations shown in Figure 6, we will isolate total muscle tissue from the animals and subject it to FACS analysis after reacting antibody against claudin 5 or ADR β 3. In this manner we will be able to quantitate the decrease in claudin 5 positive cells in the presence of cromolyn and the increase in ADR β 3 positive cells.

ii. Neuroma formation in the heterotopic bone of rats with a constricted sciatic nerve and blockade by cromolyn, capsaicin and/or ADR β 3 antagonist (L-748,337): (Months 18-36)

- a.* Since amputation in rodents does not routinely result in heterotopic ossification (HO) formation, we propose to use our BMP-induced model of HO, in conjunction with sciatic nerve restriction model.
- b.* After two weeks, bone formation will be assessed by radiographically (microCT) and bone volume quantified. Tissue will be isolated and immunostained for calcitonin gene related peptide (CGRP) and neurofilament (NF200) as well as observed for neuromas. Nerves will also be analyzed as described in the above section by immunostaining for (substance P, β Adrenergic receptor 3 (ADRB3), Ki-67(replication), human natural killer 1 (HNK1), UCP1, reelin).

See above section (Task 1i). We have not initiated the experiments using AdBMP2-transduced cells in the model using chronic gut to produce neuroma, but we have identified in our nerve defect studies, the ability generate neuromas after nerve transection, by inclusion of Adempty-transduced cells. This is extremely important and would be a means for us to follow up. Therefore, in these studies, we will not only test whether heterotopic ossification can block the neuromas formed by inclusion of the constricting the nerve with no

additions, but also determine if the compounds listed above are able to suppress both heterotopic ossification and neuroma formation. From our preliminary data suggesting that in the absence of BMP2, the adenovirus transduced cells lead to neuroma was surprising and important. This suggests that other agents and/or materials may induce neuroma in a nerve amputation setting. Indeed, in the next project period we also plan some obvious controls that have not been done, including the use of untransduced cells as well as transduction of these cells with UV-inactivated Ad Empty. Further, it suggests that if the BMP2 is close enough to the nerve, it will form heterotopic ossification around the nerve, but will not lead to neuroma. Therefore, we propose to complete these studies, with adding into the mechanism suppression by these compounds, and plan to complete this work in the next 6 months. These studies will be the focus of a publication in this area, and are extremely important since the results appear to mimic what is seen clinically in the military population particularly in the residual limbs.

Task 3: We will isolate the human counterparts of the mouse perineurial progenitor cells by fluorescence activated cell sorting using specific cell surface markers that we have shown to be present and essential for function using the mouse cells.

i. Secure DOD IRB approval (Months 0-6)

ii. Characterization of the human cells: The tissues will be serial sectioned (2 mm), and every fifth slide subject to hematoxylin and eosin staining. Serial unstained slides will be used for immunohistochemical staining integrin subunit $\alpha 3$, laminin $\beta 2$, occludin, zona occluding (ZO-1), claudins 1-5, melanoma antigen family E, member 1 (Magee1), ADRB3, β arrestin, Patched 1 (Ptch1) and 2, desert hedgehog (Dhh), smoothen (Smo), Src kinase, and UCP1. **(Months 6-36)**

c. We will also use the following combination of antibodies: ADRB3/UCP1, ADRB3/ β arrestin, β arrestin/Smo, β arrestin/Smo/Ptch1, and β arrestin/Src.

In the third aim of this application, we proposed to isolate the human equivalent of the mouse perineurial progenitor cell (2) and develop a culturing system that would enhance their expansion as well as their differentiation to transient brown adipose-like cells (2). Since human nerve tissues will not be pre-exposed to BMP2, it will be important for future clinical use of these cells to determine an optimal method for expansion, which also supports brown adipose

cell-like differentiation. These nerves were isolated fresh at the time of surgery, 5 total, by our co-investigator (ZG), placed in sterile saline, and transported immediately to the laboratory under two coordinating IRB approved protocols that cross both institutions (UTMB and BCM). Tissues were isolated during orthopedic surgeries involving amputations at UTMB (see Dr. R. Lindsey's MD letter in the original application). The human nerve tissue was washed, cut into 3-5 mm pieces quick frozen and serially sectioned at 2-15 mms in size. Some of the tissue was also fixed in buffered formalin, decalcified, processed, and paraffin embedded. Finally a subset of these tissues were subject to collagenase digestion and cells were either directly plated or subject to

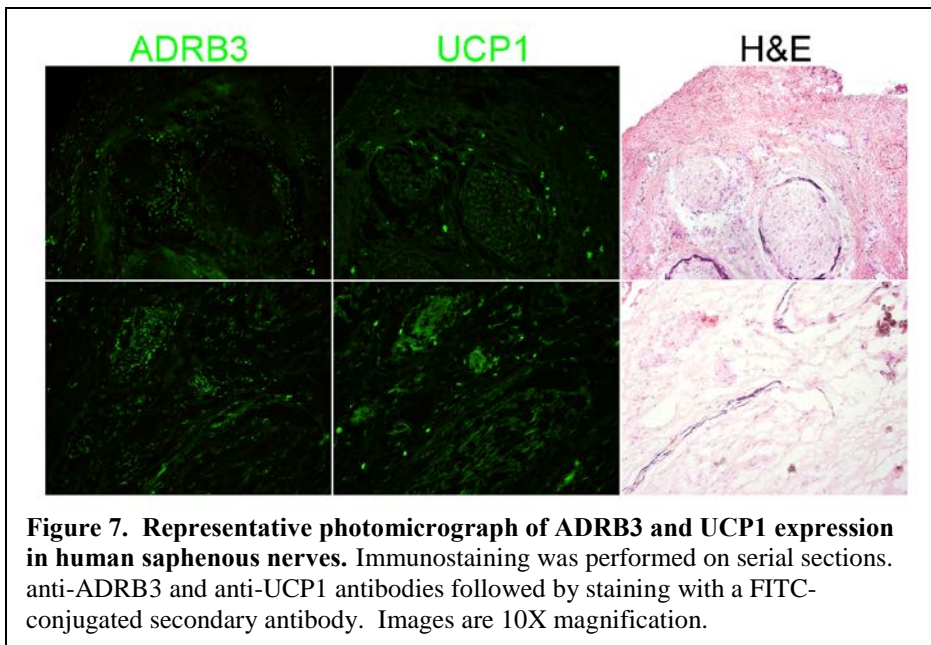


Figure 7. Representative photomicrograph of ADRB3 and UCP1 expression in human saphenous nerves. Immunostaining was performed on serial sections. anti-ADRB3 and anti-UCP1 antibodies followed by staining with a FITC-conjugated secondary antibody. Images are 10X magnification.

fluorescence activated cell sorting (FACS) for ADRB3 (see next subaim). Froze or paraffin embedded tissues, were sectioned (2 mm), and every fifth slide subjected to hematoxylin and eosin staining as previously described (4). Serial unstained slides were then used for the immunohistochemical stains depicted in Figures 7 and 8. As can be seen in figure 7, the tissues possessed the ADRB3⁺ UCP1⁺ cells that appear to co-align in the perineurial region. We previously have shown that after BMP2 induction in rodents, the progenitors within the perineurial region of peripheral nerves begin to express ADRB3 and UCP1 (2).

The perineurial fibroblasts can be seen in the corresponding hematoxylin and Eosin stained image, and stains with a purple color. Interestingly, the largest concentration of $ADRB3^+ UCP1^+$ cells appears to be in a fascicle that does

not have the purple fibroblast perineurial ring, suggesting that perhaps the perineurial cells are no longer maintaining that structure. This nerve tissue was isolated from patients that have resulted in amputation due to complications by type 2 diabetes. Both nerves also stained for UCP1 and $ADRB3$, but UCP1 seemed more retained by in the

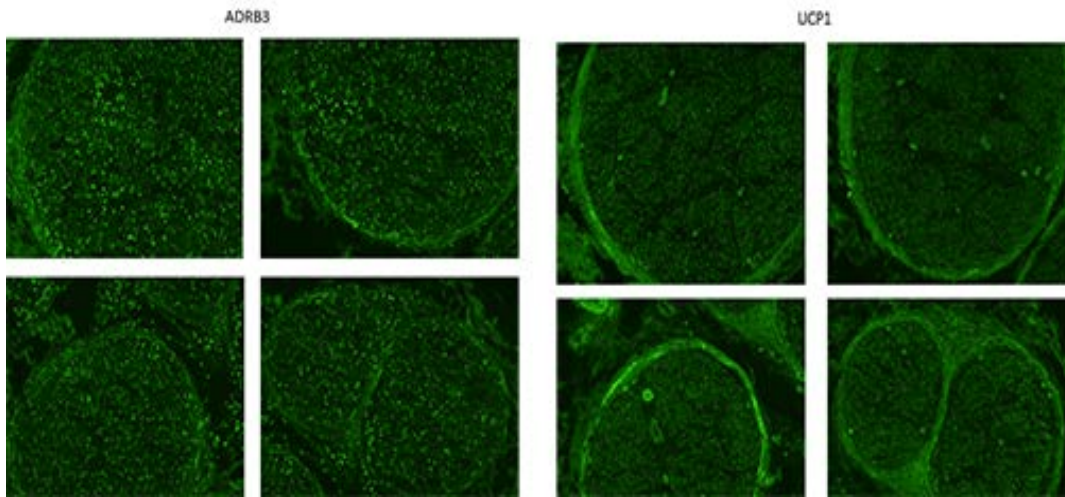


Figure 8. Neuropathic tibial human nerve expresses $ADRB3$ and $UCP1$. A tibial nerve was taken from an amputee and stained with anti- $ADRB3$ and anti- $UCP1$ antibodies followed by staining with a FITC-coniugated secondary antibody.

perineurial fibroblast layer, whereas the $ADRB3$ was more in the endoneurial compartment. This is the first time we have noted the expression of this factor in the endoneurium although recent reports suggest this may be more of a neural stem cell factor, and therefore, the activation and migration of the UCP1 brown adipocyte-like cells in the rodents, maybe ultimately derived from an earlier progenitor in the endoneurium. Alternatively, this may be related to the neuropathy; therefore, we are also noting whether the samples are derived from a type 2 diabetic patient that may have neuropathy, versus patients that do not possess this disorder. Of the 5 samples we have obtained, 2 have been from individuals with type 2 diabetes.

Immunostaining for desert hedgehog (figure 9) shows that the expression is present in the perineurial cells, in both mouse (panel A) and human (panel B). Production of desert hedgehog, presumably by Schwann cells, is a requirement for adequate perineurial formation (5). However, it is difficult for us to understand how the Schwann cell can produce desert hedgehog, since we can clearly visualize desert-hedgehog-producing cells in the perineurium of both mice and humans (figure 9), whereas the Schwann cell is in the endoneurium.

Interestingly, in the neuropathic specimen of human nerve that we obtained (Panel B) we see migration of the desert hedgehog containing cells off the perineurium and into the surrounding epineurium. This can be compared to a similar scenario in the mouse on the third day after BMP2 induction where one can see a similar migration of

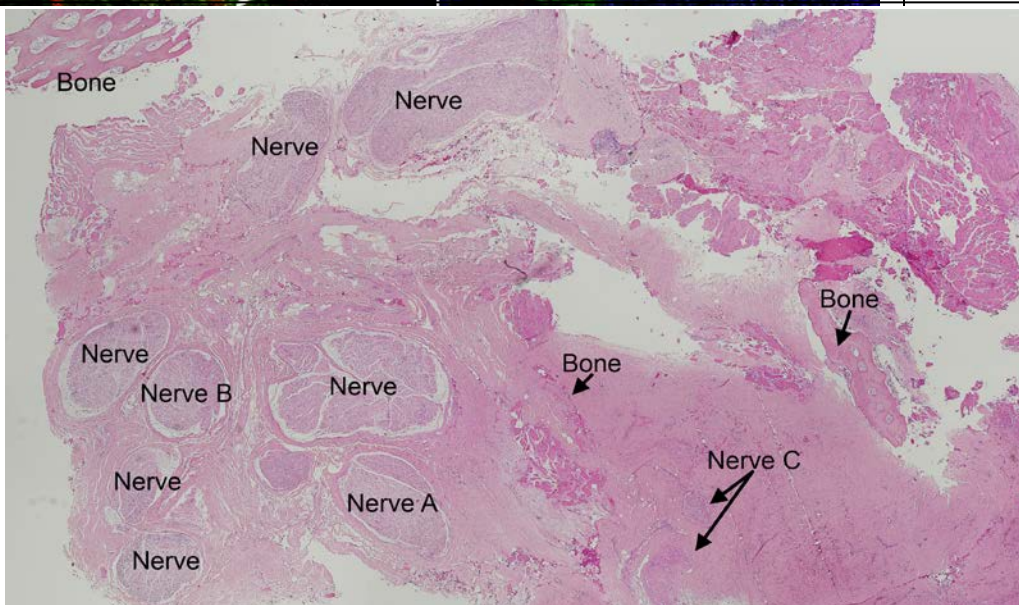


Figure 10: Montage of hematoxylin and eosin stained images, reconstructed digitally after taking the images at 4X magnification. Tissues were serially sectioned, and then analyzed and photographed. Reconstructions were done through selecting tissues which had either overlapping regions, or through our coding system that allowed us to determine how to reconstruct tissue pieces that were in separate blocks.

desert hedgehog-expressing cells off the nerve. The mouse nerve (panel A), however, is but a single fascicle and therefore the migration of these cells is directly into the muscle rather than into the epineurium as is seen in the human nerve (figure 9). This simple difference in anatomy may be very important in interpretation of studies in the mouse for both neuroma and heterotopic ossification for comparison to human. Interestingly, desert hedgehog-expressing cells have been shown to accumulate in the perineurium in neurofibromatosis caused by deletion of the neurofibromin 1 protein (6). This suggests that migration of desert hedgehog expressing cells may be a normal event for nerve remodeling, but that it is accelerated during neuroma/heterotopic ossification and is retarded during neurofibromatosis. The retardation of migration of these cells, some of which our preliminary data has shown are chondro-osseous progenitors (not shown), from the nerve may be one of the reasons that patients with neurofibromatosis are uniformly osteopenic (7).

We also have obtained tissues through a signed CRADA with the US Navy and specifically Drs. Jonathan Forsberg M.D., Ph.D. and Thomas Davis, Ph.D. Through this agreement they provided samples of human heterotopic ossification, isolated from resection of the residual limb after amputation. These individuals also had neuroma formation. This data has been shared with both Dr. Forsberg and Davis, and was presented in a recent oral presentations giving by Dr. Forsberg at the Orthopedic Research Society Annual meeting and the American Society for Bone and Mineral Research Annual Meeting. One of the samples (Figure 10) had a

significant number of nerves, which related specifically to this proposal. This image was generated from serial sections taken from the tissues. Briefly biopsies were shipped to the Davis laboratory in formalin, and were then systematically cut down to optimally fit in the cassettes for paraffin sectioning. The tissues were labelled so that they could be oriented and images reconstructed to provide a montage of a section through the complete biopsy. Figure 10 is actually a montage of over 20 microscopic fields at 4X magnification of several tissue sections that have been hematoxylin and eosin stained, that allow us to recreate the tissues. Although this is extremely time consuming, it allows us to orient the tissues with respect to nerve, potential neuroma and heterotopic bone formation. The following photomicrographs represent immunohistochemical staining of one microscopic field of the tissues focused on a single nerve, but are representative of all the nerves depicted in figure 10.

Interestingly, UCP1⁺ ADRβ3⁺ cells were found associated with the nerve similar to the other nerve tissues received from Dr. Gugala (Data not shown). However, we also

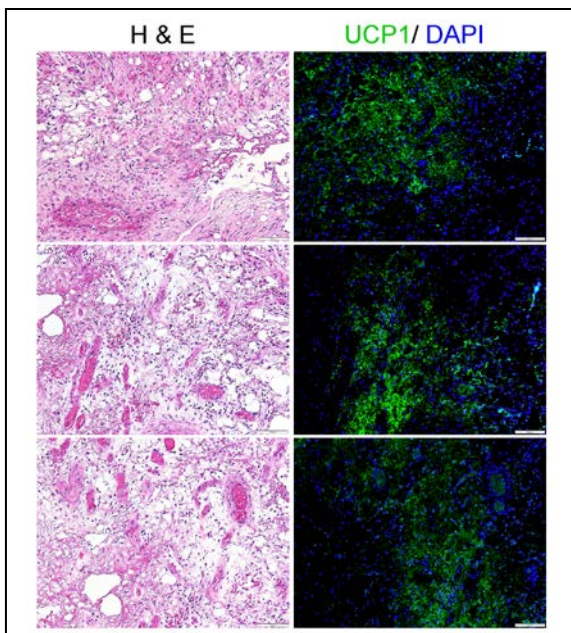


Figure 11: Representative photomicrograph of immunohistochemical staining in the tissues isolated from residual limb, in patients where amputation resulted in significant and problematic heterotopic ossification. UCP1 was identified using an antibody directed against human protein (green). Magnification 10X

noted significant UCP1⁺ brown adipocyte-like cells within the soft tissues near the heterotopic bone suggesting that the population associated with the nerve migrated from the nerve towards the new bone formation (figure 11). This is similar to what we have observed in the rodent model (Lazard et al, unpublished). We are currently continuing to characterize these tissues through immunohistochemical analysis to further compare the mechanism

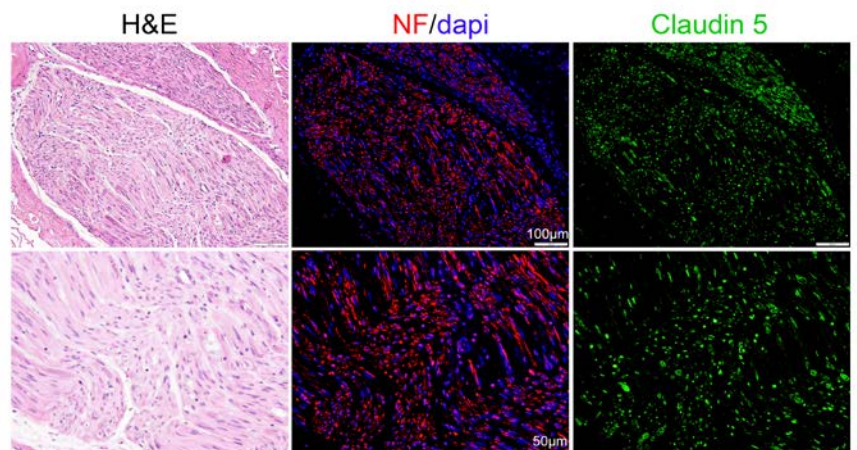


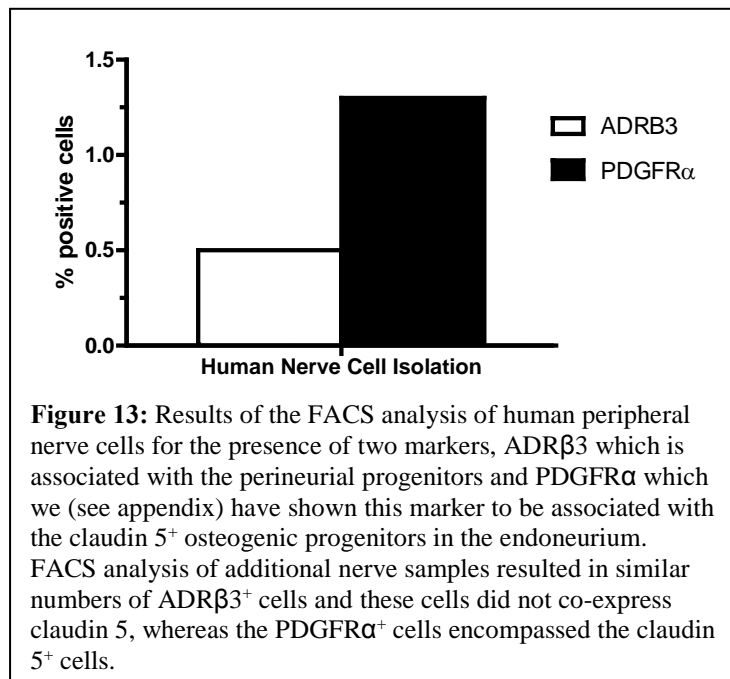
Figure 12: Representative photomicrographs of immunohistochemical staining in the tissues isolated from residual limb, in patients where amputation resulted in significant and problematic heterotopic ossification. Claudin 5 (green) and Neurofilament (red) was detected by immunohistochemistry.

identified in the mouse to these human tissues. Additionally, we have immunostained for the presence of a novel marker claudin 5, which we recently found to be associated with osteogenic progenitors derived from the endoneurium of peripheral nerves (see appendix for details about this work in mouse models of HO). As seen in figure 12, the nerves adjacent to the heterotopic bone formation expressed claudin 5 (green color) in the endoneurial compartment as determined by the positive expression of neurofilament (NF- red color), which is expressed by axons in the endoneurium. Interestingly, claudin 5 has been shown to be associated with special endothelial cells within the endoneurial vasculature (8) for contribution to the highly regulated tight junction that forms the “blood nerve barrier”. These cells have not however, been reported to be dispersed throughout the nerve endoneurium, and is intriguing since in mouse the cells rapidly leave the nerve through the specialized vasculature (see appendix). Possibly the diffusive immunostaining is representative of progenitors up-regulating claudin 5 for migration towards the bone formation, or alternatively, since the peripheral nerve signaling is disrupted through the amputation, these nerves may be reacting to both the nerve and bone injury. Alternatively, since the mouse models are staged this may represent later stages of a process that is not yet quiescent due to the amputation, and thus not identical to the mouse models in which we induce bone formation at a specific time. Therefore the studies described in task 1 are critical since they may more likely compare to these tissues, rather than the models, which don’t involve nerve injury. This work is a currently ongoing and major focus of the laboratory. We predict that a manuscript describing this data will be submitted for publication in the next two months.

iii. Isolation and culturing of human perineurial cells: Human nerve will be washed, cut into 3-5 mm pieces, fibrous epineurium will be dissected away from perineurial and endoneurial tissues digested for 20 hours at 37°C with 200 µg/ml type I collagenase and 250 µg/ml type hyaluronidase. **(Months 6-24)**

- a. Cells will be counted and either placed directly in culture or reacted with ADRB3 antibody followed by reaction with anti-human Alexa fluor 488. ADRB3⁺ will be isolated by FACS using a FACSaria II (Becton Dickenson).
- b. Cells, either before or after fluorescence activated cell sorting (FACS) selection, will be placed in neurosphere medium either unsupplemented or supplemented with 10⁻⁴ M noradrenaline, 50 ng/ml BMP2, or both. Cells will be cultured no more than two weeks and will then be characterized through immunostaining (ADRB3, UCP1, Reelin) and quantified (counting).

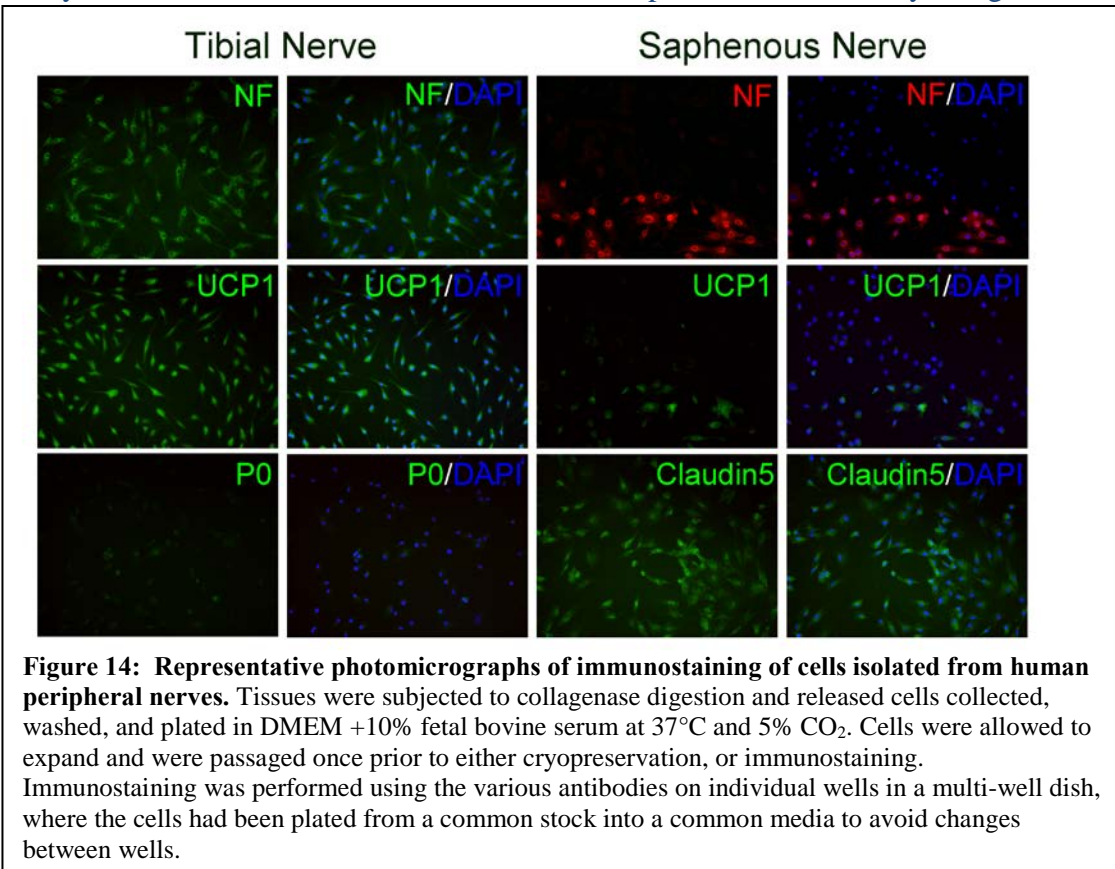
In addition to the experiments described in subaim 1, we also have isolated cells from the nerve samples



obtained by Dr. Gugala from UTMB. In these studies a portion of the nerve was digested using collagenase and cells isolated for direct culturing. With these initial studies, we did not attempt to FACS isolate the cells, but rather plated them directly for analysis. One reason for this is that we do not have a lot of lead time on when we will receive the nerve, and for some this has been either late at night or weekends, which prevents us access to the FACS core facility. Although we have attempted to isolate directly from the nerve specimens ADRB3⁺ cells (Figure 13), these were done by immunostaining the cells immediately then fixing the cells, to provide time for access to the core facility. Therefore these cells are no longer viable for culturing and animal studies, but they have been retrieved for further, immunocytochemical analysis. Those are ongoing studies to further define their phenotype with respect to the rodent cells. Further, since we would like to obtain as many samples as possible, we are switching to the

automacs system that can be performed rapidly within the laboratory. Although the cell purity is considered to be lower (85%) than with the BD FACSaria II (95%), the ability to harvest fresh cells that are enriched for the specific populations for *in vitro* and *in vivo* studies is critical.

As mentioned above, a portion of the nerve specimens have also been collagenase digested and plated directly into culture. These cells were then expanded and immunostained for the presence of ADR β 3 (figure 14). As can be seen we look at each sample and nerve type separately and figure 14 is representative of the many cell lines that were obtained from these samples and are currently being tested in our nerve defect model.



Interestingly, the majority of the cells that appeared to be digested from the tibial nerve, assumed a brown-adipocyte like phenotype under standard growth conditions in DMEM media. Alternatively only a small portion of the saphenous nerve assumed this phenotype. Although we do not believe that this is due to the type of nerve, but rather the nature of the digestion and culturing. Interestingly, claudin 5 was significantly expressed, but did not appear to overlap the UCP1⁺ cells,

suggesting that in this culture, the claudin 5⁺ cells perhaps were inadvertently selected for through digestion and culturing. We also performed immunostaining for myelin basic protein zero (P0) (figure 14), which was negative in the cells, suggesting that these cultures are not contaminated with Schwann cells. Interestingly, in both populations appeared to express neurofilament, and we are currently following up on this, using the FACS isolated cell populations that are fixed. However, we noted two separate morphologies of cells within the saphenous nerve populations all of which appeared to be claudin 5⁺ but only one morphology of the cells appears to be positive for NF. We are currently following up and completing these experiments and looking at their function in the rat nerve defect model. We will also phenotypically and functionally then compare them to the mouse population isolated under the same conditions. We are not reporting the mouse data here, because we will need to repeat the data using mouse cells isolated through automacs, rather than the FACS core facility, so that we have similar populations between mouse and human for analysis. All of the data from these experiments will be obtained within the next year.

REFERENCES:

1. Olmsted-Davis EA, Gugala Z, Gannon FH, Yotnda P, McAlhany RE, Lindsey RW, et al. Use of a chimeric adenovirus vector enhances BMP2 production and bone formation. *Human gene therapy*. 2002;13(11):1337-47. doi: 10.1089/104303402760128568. PubMed PMID: 12162816.
2. Salisbury EA, Lazard ZW, Ubogu EE, Davis AR, Olmsted-Davis EA. Transient brown adipocyte-like cells derive from peripheral nerve progenitors in response to bone morphogenetic protein 2. *Stem Cells Transl Med*. 2012;1(12):874-85. doi: 10.5966/sctm.2012-0090. PubMed PMID: 23283549; PubMed Central PMCID: PMC3659676.
3. Salisbury E, Rodenberg E, Sonnet C, Hipp J, Gannon FH, Vadakkan TJ, et al. Sensory nerve induced inflammation contributes to heterotopic ossification. *Journal of cellular biochemistry*. 2011;112(10):2748-58. doi: 10.1002/jcb.23225. PubMed PMID: 21678472; PubMed Central PMCID: PMC3329372.
4. Gugala Z, Davis AR, Foulletier-Dilling CM, Gannon FH, Lindsey RW, Olmsted-Davis EA. Adenovirus BMP2-induced osteogenesis in combination with collagen carriers. *Biomaterials*. 2007;28(30):4469-79. doi: 10.1016/j.biomaterials.2007.07.007. PubMed PMID: 17645942.

5. Parmantier E, Lynn B, Lawson D, Turmaine M, Namini SS, Chakrabarti L, et al. Schwann cell-derived Desert hedgehog controls the development of peripheral nerve sheaths. *Neuron*. 1999;23(4):713-24. PubMed PMID: 10482238.
6. Wu J, Williams JP, Rizvi TA, Kordich JJ, Witte D, Meijer D, et al. Plexiform and dermal neurofibromas and pigmentation are caused by Nf1 loss in desert hedgehog-expressing cells. *Cancer cell*. 2008;13(2):105-16. doi: 10.1016/j.ccr.2007.12.027. PubMed PMID: 18242511; PubMed Central PMCID: PMC2846699.
7. Brunetti-Pierrri N, Doty SB, Hicks J, Phan K, Mendoza-Londono R, Blazo M, et al. Generalized metabolic bone disease in Neurofibromatosis type I. *Molecular genetics and metabolism*. 2008;94(1):105-11. doi: 10.1016/j.ymgme.2007.12.004. PubMed PMID: 18289904; PubMed Central PMCID: PMC2430595.
8. Yosef N, Xia RH, Ubogu EE. Development and characterization of a novel human in vitro blood-nerve barrier model using primary endoneurial endothelial cells. *Journal of neuropathology and experimental neurology*. 2010;69(1):82-97. doi: 10.1097/NEN.0b013e3181c84a9a. PubMed PMID: 20010300.
9. Pittenger MF, Mackay AM, Beck SC, Jaiswal RK, Douglas R, Mosca JD, et al. Multilineage potential of adult human mesenchymal stem cells. *Science*. 1999;284(5411):143-7. PubMed PMID: 10102814.
10. Suda RK, Billings PC, Egan KP, Kim JH, McCarrick-Walmsley R, Glaser DL, et al. Circulating osteogenic precursor cells in heterotopic bone formation. *Stem cells*. 2009;27(9):2209-19. doi: 10.1002/stem.150. PubMed PMID: 19522009; PubMed Central PMCID: PMC3496263.
11. Kumagai K, Vasanji A, Drazba JA, Butler RS, Muschler GF. Circulating cells with osteogenic potential are physiologically mobilized into the fracture healing site in the parabiotic mice model. *Journal of orthopaedic research : official publication of the Orthopaedic Research Society*. 2008;26(2):165-75. doi: 10.1002/jor.20477. PubMed PMID: 17729300.
12. Otsuru S, Tamai K, Yamazaki T, Yoshikawa H, Kaneda Y. Circulating bone marrow-derived osteoblast progenitor cells are recruited to the bone-forming site by the CXCR4/stromal cell-derived factor-1 pathway. *Stem cells*. 2008;26(1):223-34. doi: 10.1634/stemcells.2007-0515. PubMed PMID: 17932420.
13. Medici D, Shore EM, Lounev VY, Kaplan FS, Kalluri R, Olsen BR. Conversion of vascular endothelial cells into multipotent stem-like cells. *Nature medicine*. 2010;16(12):1400-6. doi: 10.1038/nm.2252. PubMed PMID: 21102460; PubMed Central PMCID: PMC3209716.
14. Lounev VY, Ramachandran R, Wosczyzna MN, Yamamoto M, Maidment AD, Shore EM, et al. Identification of progenitor cells that contribute to heterotopic skeletogenesis. *The Journal of bone and joint surgery American volume*. 2009;91(3):652-63. doi: 10.2106/JBJS.H.01177. PubMed PMID: 19255227; PubMed Central PMCID: PMC2663346.
15. Wosczyzna MN, Biswas AA, Cogswell CA, Goldhamer DJ. Multipotent progenitors resident in the skeletal muscle interstitium exhibit robust BMP-dependent osteogenic activity and mediate heterotopic ossification. *J Bone Miner Res*. 2012;27(5):1004-17. Epub 2012/02/07. doi: 10.1002/jbmr.1562. PubMed PMID: 22307978; PubMed Central PMCID: PMC3361573.
16. Cairns DM, Liu R, Sen M, Canner JP, Schindeler A, Little DG, et al. Interplay of Nkx3.2, Sox9 and Pax3 regulates chondrogenic differentiation of muscle progenitor cells. *PloS one*. 2012;7(7):e39642. doi: 10.1371/journal.pone.0039642. PubMed PMID: 22768305; PubMed Central PMCID: PMC3388093.
17. Jackson WM, Aragon AB, Bulken-Hoover JD, Nesti LJ, Tuan RS. Putative heterotopic ossification progenitor cells derived from traumatized muscle. *Journal of orthopaedic research : official publication of the Orthopaedic Research Society*. 2009;27(12):1645-51. doi: 10.1002/jor.20924. PubMed PMID: 19517576; PubMed Central PMCID: PMC3014572.
18. Polfer EM, Forsberg JA, Fleming ME, Potter BK. Neurovascular entrapment due to combat-related heterotopic ossification in the lower extremity. *The Journal of bone and joint surgery American volume*. 2013;95(24):e195(1-6). doi: 10.2106/JBJS.M.00212. PubMed PMID: 24352781.
19. Pringle N, Collarini EJ, Mosley MJ, Heldin CH, Westermark B, Richardson WD. PDGF A chain homodimers drive proliferation of bipotential (O-2A) glial progenitor cells in the developing rat optic nerve. *The EMBO journal*. 1989;8(4):1049-56. PubMed PMID: 2545439; PubMed Central PMCID: PMC400913.
20. Richardson WD, Pringle N, Mosley MJ, Westermark B, Dubois-Dalcq M. A role for platelet-derived growth factor in normal gliogenesis in the central nervous system. *Cell*. 1988;53(2):309-19. PubMed PMID: 2834067.
21. Su EJ, Fredriksson L, Geyer M, Folestad E, Cale J, Andrae J, et al. Activation of PDGF-CC by tissue plasminogen activator impairs blood-brain barrier integrity during ischemic stroke. *Nature medicine*. 2008;14(7):731-7. doi: 10.1038/nm1787. PubMed PMID: 18568034; PubMed Central PMCID: PMC2811427.
22. Gugala Z, Olmsted-Davis EA, Gannon FH, Lindsey RW, Davis AR. Osteoinduction by ex vivo adenovirus-mediated BMP2 delivery is independent of cell type. *Gene therapy*. 2003;10(16):1289-96. doi: 10.1038/sj.gt.3302006. PubMed PMID: 12883525.
23. Fouletier-Dilling CM, Bosch P, Davis AR, Shafer JA, Stice SL, Gugala Z, et al. Novel compound enables high-level adenovirus transduction in the absence of an adenovirus-specific receptor. *Human gene therapy*. 2005;16(11):1287-97. doi: 10.1089/hum.2005.16.1287. PubMed PMID: 16259562.
24. Fouletier-Dilling CM, Gannon FH, Olmsted-Davis EA, Lazard Z, Heggenes MH, Shafer JA, et al. Efficient and rapid osteoinduction in an immune-competent host. *Human gene therapy*. 2007;18(8):733-45. doi: 10.1089/hum.2006.190. PubMed PMID: 17691858.
25. Olmsted-Davis E, Gannon FH, Ozen M, Ittmann MM, Gugala Z, Hipp JA, et al. Hypoxic adipocytes pattern early heterotopic bone formation. *The American journal of pathology*. 2007;170(2):620-32. doi: 10.2353/ajpath.2007.060692. PubMed PMID: 17255330; PubMed Central PMCID: PMC1851874.
26. Kan L, Lounev VY, Pignolo RJ, Duan L, Liu Y, Stock SR, et al. Substance P signaling mediates BMP-dependent heterotopic ossification. *Journal of cellular biochemistry*. 2011;112(10):2759-72. doi: 10.1002/jcb.23259. PubMed PMID: 21748788; PubMed Central PMCID: PMC3508732.

27. Nakashima K, Zhou X, Kunkel G, Zhang Z, Deng JM, Behringer RR, et al. The novel zinc finger-containing transcription factor osterix is required for osteoblast differentiation and bone formation. *Cell*. 2002;108(1):17-29. PubMed PMID: 11792318.
28. Mizisin AP, Weerasuriya A. Homeostatic regulation of the endoneurial microenvironment during development, aging and in response to trauma, disease and toxic insult. *Acta neuropathologica*. 2011;121(3):291-312. doi: 10.1007/s00401-010-0783-x. PubMed PMID: 21136068; PubMed Central PMCID: PMC3038236.
29. Weerasuriya A, Mizisin AP. The blood-nerve barrier: structure and functional significance. *Methods in molecular biology*. 2011;686:149-73. doi: 10.1007/978-1-60761-938-3_6. PubMed PMID: 21082370.
30. Yosef N, Ubogu EE. An immortalized human blood-nerve barrier endothelial cell line for in vitro permeability studies. *Cellular and molecular neurobiology*. 2013;33(2):175-86. doi: 10.1007/s10571-012-9882-7. PubMed PMID: 23104242; PubMed Central PMCID: PMC3568212.
31. Ubogu EE. The molecular and biophysical characterization of the human blood-nerve barrier: current concepts. *Journal of vascular research*. 2013;50(4):289-303. doi: 10.1159/000353293. PubMed PMID: 23839247; PubMed Central PMCID: PMC4030640.
32. Nitta T, Hata M, Gotoh S, Seo Y, Sasaki H, Hashimoto N, et al. Size-selective loosening of the blood-brain barrier in claudin-5-deficient mice. *The Journal of cell biology*. 2003;161(3):653-60. doi: 10.1083/jcb.200302070. PubMed PMID: 12743111; PubMed Central PMCID: PMC2172943.
33. Cosgaya JM, Chan JR, Shooter EM. The neurotrophin receptor p75NTR as a positive modulator of myelination. *Science*. 2002;298(5596):1245-8. doi: 10.1126/science.1076595. PubMed PMID: 12424382.
34. Morrison SJ, White PM, Zock C, Anderson DJ. Prospective identification, isolation by flow cytometry, and in vivo self-renewal of multipotent mammalian neural crest stem cells. *Cell*. 1999;96(5):737-49. PubMed PMID: 10089888.
35. Kazmierski R, Michalak S, Wencel-Warot A, Nowinski WL. Serum tight-junction proteins predict hemorrhagic transformation in ischemic stroke patients. *Neurology*. 2012;79(16):1677-85. doi: 10.1212/WNL.0b013e31826e9a83. PubMed PMID: 22993287.
36. Rampon C, Weiss N, Deboux C, Chaverot N, Miller F, Buchet D, et al. Molecular mechanism of systemic delivery of neural precursor cells to the brain: assembly of brain endothelial apical cups and control of transmigration by CD44. *Stem cells*. 2008;26(7):1673-82. doi: 10.1634/stemcells.2008-0122. PubMed PMID: 18450824.
37. Nakamura M, Okano H, Blendy JA, Montell C. Musashi, a neural RNA-binding protein required for Drosophila adult external sensory organ development. *Neuron*. 1994;13(1):67-81. PubMed PMID: 8043282.
38. Okano H, Kawahara H, Toriya M, Nakao K, Shibata S, Imai T. Function of RNA-binding protein Musashi-1 in stem cells. *Experimental cell research*. 2005;306(2):349-56. doi: 10.1016/j.yexcr.2005.02.021. PubMed PMID: 15925591.
39. Battelli C, Nikopoulos GN, Mitchell JG, Verdi JM. The RNA-binding protein Musashi-1 regulates neural development through the translational repression of p21WAF-1. *Molecular and cellular neurosciences*. 2006;31(1):85-96. doi: 10.1016/j.mcn.2005.09.003. PubMed PMID: 16214366.
40. Eccleston PA, Funari K, Heldin CH. Expression of platelet-derived growth factor (PDGF) and PDGF alpha- and beta-receptors in the peripheral nervous system: an analysis of sciatic nerve and dorsal root ganglia. *Developmental biology*. 1993;155(2):459-70. doi: 10.1006/dbio.1993.1044. PubMed PMID: 8432400.
41. Saharinen P, Eklund L, Miettinen J, Wirkkala R, Anisimov A, Winderlich M, et al. Angiopoietins assemble distinct Tie2 signalling complexes in endothelial cell-cell and cell-matrix contacts. *Nature cell biology*. 2008;10(5):527-37. doi: 10.1038/ncb1715. PubMed PMID: 18425119.
42. Escudero-Esparza A, Jiang WG, Martin TA. Claudin-5 is involved in breast cancer cell motility through the N-WASP and ROCK signalling pathways. *Journal of experimental & clinical cancer research : CR*. 2012;31:43. doi: 10.1186/1756-9966-31-43. PubMed PMID: 22559840; PubMed Central PMCID: PMC3432004.
43. Asahara T, Murohara T, Sullivan A, Silver M, van der Zee R, Li T, et al. Isolation of putative progenitor endothelial cells for angiogenesis. *Science*. 1997;275(5302):964-7. PubMed PMID: 9020076.
44. Dilling CF, Wada AM, Lazard ZW, Salisbury EA, Gannon FH, Vadakkan TJ, et al. Vessel formation is induced prior to the appearance of cartilage in BMP-2-mediated heterotopic ossification. *Journal of bone and mineral research : the official journal of the American Society for Bone and Mineral Research*. 2010;25(5):1147-56. doi: 10.1359/jbmr.091031. PubMed PMID: 19839764; PubMed Central PMCID: PMC3153372.
45. DeGrendele HC, Estess P, Picker LJ, Siegelman MH. CD44 and its ligand hyaluronate mediate rolling under physiologic flow: a novel lymphocyte-endothelial cell primary adhesion pathway. *The Journal of experimental medicine*. 1996;183(3):1119-30. PubMed PMID: 8642254; PubMed Central PMCID: PMC2192320.
46. DeGrendele HC, Estess P, Siegelman MH. Requirement for CD44 in activated T cell extravasation into an inflammatory site. *Science*. 1997;278(5338):672-5. PubMed PMID: 9381175.
47. Gerber HP, Vu TH, Ryan AM, Kowalski J, Werb Z, Ferrara N. VEGF couples hypertrophic cartilage remodeling, ossification and angiogenesis during endochondral bone formation. *Nature medicine*. 1999;5(6):623-8. doi: 10.1038/9467. PubMed PMID: 10371499.
48. Oberlin E, Amara A, Bachelier F, Bessia C, Virelizier JL, Arenzana-Seisdedos F, et al. The CXC chemokine SDF-1 is the ligand for LESTR/fusin and prevents infection by T-cell-line-adapted HIV-1. *Nature*. 1996;382(6594):833-5. doi: 10.1038/382833a0. PubMed PMID: 8752281.
49. Wagner DD, Frenette PS. The vessel wall and its interactions. *Blood*. 2008;111(11):5271-81. doi: 10.1182/blood-2008-01-078204. PubMed PMID: 18502843; PubMed Central PMCID: PMC2396724.

50. Decker B, Bartels H, Decker S. Relationships between endothelial cells, pericytes, and osteoblasts during bone formation in the sheep femur following implantation of tricalciumphosphate-ceramic. *The Anatomical record*. 1995;242(3):310-20. doi: 10.1002/ar.1092420304. PubMed PMID: 7573978.
51. Mishina Y, Snider TN. Neural crest cell signaling pathways critical to cranial bone development and pathology. *Experimental cell research*. 2014. doi: 10.1016/j.yexcr.2014.01.019. PubMed PMID: 24509233.
52. Garcia-Castro MI, Marcelle C, Bronner-Fraser M. Ectodermal Wnt function as a neural crest inducer. *Science*. 2002;297(5582):848-51. PubMed PMID: 12161657.
53. Lee HY, Kleber M, Hari L, Brault V, Suter U, Taketo MM, et al. Instructive role of Wnt/beta-catenin in sensory fate specification in neural crest stem cells. *Science*. 2004;303(5660):1020-3. doi: 10.1126/science.1091611. PubMed PMID: 14716020.
54. Kleber M, Lee HY, Wurdak H, Buchstaller J, Riccomagno MM, Ittner LM, et al. Neural crest stem cell maintenance by combinatorial Wnt and BMP signaling. *The Journal of cell biology*. 2005;169(2):309-20. doi: 10.1083/jcb.200411095. PubMed PMID: 15837799; PubMed Central PMCID: PMC2171862.
55. Sullivan MP, Torres SJ, Mehta S, Ahn J. Heterotopic ossification after central nervous system trauma: A current review. *Bone & joint research*. 2013;2(3):51-7. doi: 10.1302/2046-3758.23.2000152. PubMed PMID: 23610702; PubMed Central PMCID: PMC3626201.
56. Shlosberg D, Benifla M, Kaufer D, Friedman A. Blood-brain barrier breakdown as a therapeutic target in traumatic brain injury. *Nature reviews Neurology*. 2010;6(7):393-403. doi: 10.1038/nrneuro.2010.74. PubMed PMID: 20551947; PubMed Central PMCID: PMC3625732.

- **Training**

This project was really not intended to provide training or professional development. However, there is one over-riding theme that we think drives home an important lesson. This project, on the problem of neuroma in injury to soldiers, is an important example of cross-disciplinary research. Frequently scientists are pigeon-holed into specific areas of research, and often it is believed that “specializing” in a given discipline may be an important aspect of scientific training. However, the human body often uses several organ systems and tissues acting in unison for certain functions. Therefore it may also be useful to consider a “systems” approach to understanding these processes. We have found that heterotopic ossification is indeed such a process, with nerves, vessels, and fat all playing a role in addition to that of the bone cells themselves. Thus far the results of this project have been striking, in that neuroma appears to be not only a defect in the nerve, but also a defect in the signal calling for bone formation, this signal being incomplete or defective when neuromas form.

- **Dissemination of results**

We have only recently obtained the results described in this report and they have not yet been disseminated. After repetition of key experiments to assure their validity, these results will be submitted to a high quality medical journal for peer-reviewed publication. This is, of course, the first-line and most important forum for initial distribution of important results in medical research. Some of these results were presented in abbreviated form at the ASBMR meeting, Houston, TX 2014.

- **Plans for next reporting period**

1. Repeat key experiments and publish results
2. Our results indicate that neuromas form when cells transduced with control (empty) adenovirus are delivered in the area of cut nerves. We would like to see if treatment, either before or at the same time as delivery of these transduced cells, will have an effect on neuroma formation.
 - a. Sodium cromolyn
 - b. Capsaicin
 - c. Antagonists of the β_3 adrenergic receptor

We plan to report on these experiments when we provide the next progress report. In addition, several of the results described in this report deserve further investigation.

IMPACT

The results described in this report show that heterotopic ossification and neuroma are different parts of the same process. The results also point the way toward preventing and treating neuroma.

CHANGES/PROBLEMS

Nothing to report

PRODUCTS

Conference presentation: American Society of Bone and Mineral Research Annual Meeting, Houston, TX 77030

PARTICIPANTS & OTHER COLLABORATING ORGANIZATIONS

Name:	Alan R. Davis
Project Role:	Principle Investigator
Researcher Identifier:	043833
Nearest persons month worked:	1.8 months
Contribution to Project:	Oversees all aspects of the award, and involved directly with working with post-doctoral fellow to design and conduct experiments
Funding Source:	Grant award

Name:	Elizabeth Olmsted-Davis
Project Role:	Co-Investigator
Researcher Identifier:	043834
Nearest persons month worked:	1.8 months
Contribution to Project:	Works with post-doctoral fellow on data collection and analysis
Funding Source:	Grant award

Name:	Zibi Gugala
Project Role:	Co-Investigator
Researcher Identifier:	042482
Nearest persons month worked:	1 calendar month
Contribution to Project:	Provides nerve tissues, and support for human nerve studies
Funding Source:	Subcontract

Name:	Eroboghene Ubogu
Project Role:	Co-investigator
Researcher Identifier:	
Nearest persons month worked:	1 month
Contribution to Project:	Provides neurological data interpretation, insites for experimental planning, and also review of all materials such as posters and manuscript preparation
Funding Source:	Subcontract

Name:	Elizabeth Salisbury
Project Role:	Post-Doctoral Fellow
Researcher Identifier:	14620
Nearest persons month worked:	3 months
Contribution to Project:	Conducted the experiments and collected data as described in this report
Funding Source:	Departmental Funds

Name:	Pedro Alvarez-Urena
Project Role:	Post-Doctoral Fellow
Researcher Identifier:	186161
Nearest persons month worked:	3 calendar months
Contribution to Project:	Currently conducting the nerve and neuroma experiments, including all the experiments described above, that are listed as ongoing.
Funding Source:	Grant award

Name:	ZaWaunyka Lazard
Project Role:	Research Technician
Researcher Identifier:	039764
Nearest persons month worked:	3 months
Contribution to Project:	Conducted and oversees the rodent animal experiments and maintains the colony
Funding Source:	Departmental funds

Changes in research personnel:

One of the major changes is that Dr. Erobohene Ubogu , M.D. Ph.D. has moved to University of Alabama as there chairman of neurology, and thus is no longer at BCM. Dr. Ubogu, continues to work with the PI and co-investigators on the proposed experiments and has agreed to return to BCM to conduct the electrical conductance studies, however, the funds within the grant dedicated for these studies, must now be sub-contracted back to Dr. Ubogu. BCM has been working on requesting this subcontract from the Department of Defense and we request that this be favorably considered, since he has been instrumental in the development of this project, and has significant interest in continuing his involvement. Further, he is critical for completion of the award.

Additionally Dr. Salisbury, Ph.D. is currently transistioning to a faculty position as an independent investigator so we have hired Dr. Pedro Alvarez-Urena, Ph.D. to take over the work. Dr. Alvarez-Urena, just received his Ph.D. degree from Carnegie Mellon University in the laboratory of Dr. Jeffery Hollinger, and has substantial background in both heterotopic ossification and bone tissue engineering. Although he has not been involved in studies involving the role of peripheral nerves, he approached us for a post-doctoral fellowship, because of his specific interests in this area.

What other organizations were involved as partners:

Medical Branch of University of Texas (UTMB) in Galveston, TX

Contributions: They have been instrumental in providing the human tissues for these studies. Dr. Gugala (who is currently the recipient of a subcontract on the award) currently has an IRB approved protocol for this work, that is linked to the BCM IRB approved protocol, allow for Dr. Gugala to obtain the tissues, and transport them to research personnel (Dr. Salisbury, and Dr. Alvarez-Urena) in the Davis laboratory for further dissection and studies.

University of Alabama (UAB) at Birmingham

Contributions: Dr. Ubogu has committed both intellectual time, in reviewing the data and discussions of the directions and/or troubleshooting of the experiments, but he will also be providing data collection through performing all the electrical conductance experiments. Dr. Ubogu was originally earmarked a portion of the budget, that was received by BCM, however, since he has moved, we hope to provide these funds through a subcontract.

SPECIAL REPORTING REQUIREMENTS: Not applicable.

APPENDICES:

Neural Origin of Osteoblasts during Heterotopic Ossification

ZaWaunyka W Lazard¹, Elizabeth A. Olmsted-Davis^{1,2,3}, Elizabeth A Salisbury¹, Zbigniew Gugala⁴, Eric Beal II¹, Rita P. Nistal¹, Erobohene H. Ubogu⁵, and Alan R. Davis^{1,2,3}

Center for Cell and Gene Therapy¹, Departments of Pediatrics, Hematology-Oncology² and
Orthopedic Surgery³

Baylor College of Medicine

One Baylor Plaza

Houston, TX 77030

Department of Orthopedic Surgery and Rehabilitation⁴

University of Texas

School of Medicine

Galveston, TX 77555

Department of Neurology⁵

The University of Alabama at Birmingham

Birmingham, AL 35294

Bone morphogenetic protein type 2/heterotopic ossification/claudin 5/tight junctional molecules/blood-
nerve barrier/blood-brain barrier/extravasation

Abstract

Introduction: Heterotopic ossification (HO) is the process of *de novo* bone formation at a non-skeletal site.

Recently, we showed that the earliest steps in this process involve changes in sensory nerves. Here, we extend these studies by identifying unique osteogenic progenitors within the endoneurial compartment of

nerves adjacent to the site of HO after delivery of sustained low-levels of bone morphogenetic protein type 2 (BMP2).

Materials and Methods: HO was induced by intramuscular injection of Ad5BMP2-transduced cells in mice. Osteoprogenitors were identified through immunohistochemistry then quantified and further characterized by fluorescence activated cell sorting (FACS) and immunocytochemistry.

Results: Induction of HO by low-dose BMP2 leads to the expression, within 24 h, of the osteoblast-specific transcription factors, *dlx5* and osterix in osteoprogenitors in the endoneurium of local peripheral nerves. This is then followed by their coordinate disappearance from the nerve and re-appearance in the circulation by 48 hours. During their exit from the nerve, these cells begin to express the tight junction molecule, claudin 5. These osterix⁺ claudin 5⁺ cells then disappear from circulation approximately 3-4 days after delivery of BMP2 followed by coordinate reappearance at the site of bone formation. Concurrent with this reappearance, we observed significant elevated expression of factors involved in extravasation (CXCR4, E-selectin, and CD44) These endoneurial progenitors also expressed the neural markers PDGFR α , the low-affinity nerve growth factor receptor (p75(NTR) and the neural crest stem cell marker musashi-1 as well as the endothelial marker Tie-2. They were distinct from the perineurial-like progenitors we previously described that form the transient brown adipocytes (2).

Conclusions: We conclude that these endoneurial progenitors are osteogenic precursors that are utilized for heterotopic ossification.

Introduction

Osteoblasts have long been thought to be uniquely derived from the bone marrow mesenchymal stem cells (9). However, several alternate mechanisms have recently been noted including the description of circulating osteoprogenitors that are osteocalcin⁺ and osteopontin⁺ (10-12) as well as the presence of osteoprogenitors that take on the characteristics of endothelial cells before being incorporated as osteoblasts in heterotopic ossification (13). Recent studies suggest the presence of a local stem/progenitor cell that could become a fully differentiated osteoblast in models of heterotopic ossification (HO) (13, 14) (3). Initial reports of such a localized osteoprogenitor suggested that it may be a muscle satellite (15) or smooth muscle cell (16), which in the presence of BMP2, expands and undergoes osseous differentiation. However, Lounev *et al*, through lineage tracing for the hematopoietic-endothelial marker Tie-2, demonstrated the presence of reporter in the immature fibroproliferative cells as well as the osteogenic cells within HO, suggesting that the cells were endothelial in origin (14). They also found that the smooth muscle marker, smooth muscle myosin heavy chain (SMMHC) and skeletal muscle marker (MyoD) were observed in less than 5% of the cells. Opposing this theory, Wosczyzna *et al* using a similar lineage tracing system, suggested that the Tie-2⁺ PDGFR α ⁺ Sca-1⁺ myoD⁻ progenitor is distinct from the vascular endothelium and resides in the interstitial region of skeletal muscle (15). They demonstrated that the native endothelial cells did not participate in HO, nor did exogenously delivered endothelial cells previously exposed to BMP2. Setting them apart from previously described muscle stem cell populations, these progenitors were negative for myoD, pericyte markers, did not share a basal lamina with the adjacent endothelium, and appeared to be a totally distinct cell population.

In support of these findings, studies of human heterotopic ossification in the military population suggest the presence of a mesenchymal stem cell expressing PDGFR α (17). Furthermore, HO observed in military patients often involves or encompasses the peripheral nerves, termed neurovascular entrapment, making it difficult to surgically remove (18). However, all studies agree that the progenitor possesses the neural/glial cell-specific receptor PDGFR α (19, 20) (21).

We previously demonstrated a link between peripheral nerves and HO in a murine model, which relies on sustained delivery of BMP2 through injection of AdBMP2- transduced cells into muscle (3). Although these cells are rapidly cleared within four days, they express low levels of BMP2, at a maximum 50 ng total, and launch a series of events that leads to mineralized bone within 7 days (1) (22) (23) (24). Salisbury *et al* (3)

identified the immediate expression of the pain mediators, substance P and GCRP, upon delivery of the BMP2, which leads to neural inflammation with resultant degranulation of local mast cells and remodeling of the epineurium. Removal of the epineurium was correlated with migration of progenitors that reside in the perineurium that undergo brown adipogenesis (2), presumably for the purpose of patterning the new bone (25). Blocking this process either through delivery of inhibitors of mast cell degranulation (3) or binding of pain mediators to their receptor (26) resulted in a significant decrease in HO. Blocking nerve remodeling led to the accumulation within the endoneurium of *nanog*⁺ *Klf-4*⁺ *osterix*⁺ progenitors (27).

The endoneurium contains the axons and their supporting glial cells, called Schwann cells, embedded in loose collagen fibrils within unique fascicles surrounded by multiple layers of perineurial cells (28, 29). The endoneurium possesses a tight junction forming microvascular barrier similar to that found in the brain. This barrier is critical in control of the endoneurial microenvironment needed to maintain normal axonal signal transduction and is known as the blood-nerve barrier (BNB) (30). An important protein, claudin 5, has been shown to be an essential component of restrictive microvascular barriers. This protein is expressed at sites of cell-to-cell contact on human endoneurial endothelial cells *in vitro* (8) (31). Mice lacking expression of claudin 5 lack a functional blood-brain barrier (BBB) and die immediately after birth (32).

Here we extend these studies to further characterize the *osterix*⁺ cells residing in nerve to determine if they are derived from stem and/or progenitor cells within the endoneurium or from pre-existing differentiated cells, such as endothelial or Schwann cells, which also reside in this region. These studies suggest that a neural progenitor resides within the endoneurial compartment of local peripheral nerves that starts to express *osterix* and rapidly migrates through the tight junction of the nerve into the circulation allowing it to home to the site of newly forming bone. Thus, our data supports both the presence of localized progenitors as well as a circulating cell and provides a novel connection between heterotopic ossification and sensory nerves.

Materials and Methods

Cell Culture: A murine fibroblast cell line was obtained from the American Type Culture Collection (Manassas, VA) and propagated in α -minimum essential medium (α -MEM). This cell type is not capable of inducing bone formation before transduction. The cell line was supplemented with 10% fetal bovine serum (HyClone, Logan,, UT), penicillin (100 units/mL), streptomycin (100 μ g/mL) and amphotericin B (25 μ g/mL) (Invitrogen Life Technologies, Gaithersburg, MD). The cell line was grown at 37°C and 5% CO₂ in humidified air.

Heterotopic Bone Assay: Replication defective E1- to E3- deleted human adenovirus type 5 fiber protein (Ad5) was constructed to contain cDNAs for BMP2 in the E1 region of the virus (1) or did not contain any transgene in this region, Ad Empty. The resultant purified viruses, AdBMP2 and Ad Empty cassette, had viral particle(VP)-to-plaque-forming unit (PFU) ratios of 1:77 and 1:111, respectively, and all viruses were confirmed to be negative for replication competent adenovirus (1). Cells were transduced as previously described with AdBMP2 or Ad Empty cassette at a viral concentration of 5,000VP/cell with 1.2% Gene Jammer (23) (24). MC3T3-E1 cells lack the receptor for Ad5, the coxsackievirus-adenovirus receptor (CAR) and therefore GeneJammer is used to efficiently transduce the cells. Adenovirus was allowed to incubate overnight at 37°C, humidified atmosphere and 5% CO₂. The transduced cells were resuspended at a concentration of 5x10⁶ cells per 100 μ L of PBS and delivered by intramuscular injection into the hind limb quadriceps muscle of C57BL/6 (Jackson Laboratory Repository, Bar Harbor, ME).

Immunohistological and immunocytochemical analysis: For paraffin sections the entire hind limb including the skeletal bone was harvested, the skin was removed, then the tissue was decalcified and paraffin embedded. For frozen sections the soft tissue encompassing the site of the new bone formation were isolated from the rear hind limbs and flash frozen. Serial sections (3-4 μ m) were prepared with approximately 50 sections per tissue specimen. Hematoxylin and eosin staining was performed on every tenth slide in order to locate the region containing our delivery cells or the newly forming endochondral bone. Serial unstained slides were used for immunohistochemical staining with either single or double antibody labeling. Primary antibodies were added to slides at a dilution of 1:100 to 1:200 with an overnight incubation, washed and incubated with respective secondary antibodies of either Alexa Fluor 488, 594 or 647 (Invitrogen Life Technologies) at a 1:500 dilution. Primary antibodies were used as follows: Claudin 5 (Novus Biological), CD31 (BD Pharmingen), Neurofilament (NF) (Sigma-Aldrich), osterix (OSX) (R & D systems), Tie 2 (Chemicon), *dlx 5* (Santa Cruz),

[CD44, E-selectin (CD62), myelin protein 0 (p0), Musashi 1 (NRP-1), nerve growth factor receptor (NGF, p75)] [Abcam]. Primary and secondary antibodies were diluted in 2% bovine serum albumin or the mouse on mouse, M.O.M. kit, (Vector Laboratories) was used according to manufacturer protocol for mouse antibodies. Tissues were counterstained and covered with Vectashield mounting medium containing DAPI (Vector Laboratories).

Cytospin slide preparations of FACS isolated cells were produced by centrifugation of approximately 40,000 cells at 500 rpm, using a Cytopro 7620 cytocentrifuge (Wescor), for 5 minutes. The slides were subsequently immunostained following similar methods as above. Briefly, cells were fixed with 4% paraformaldehyde, PBS washed, treated with 0.3% Triton X-100 in 0.3% Tris-buffered saline, blocked with 2% BSA, and incubated in primary antibody overnight. After PBS washing, samples were incubated in the appropriate secondary antibody and counterstained with DAPI. Stained cells were examined by confocal microscopy (LSM 510 META, Zeiss, Inc.).

Flow Cytometry and Fluorescence Activated Cell Sorting (FACS): Cells isolated from the hind limb soft tissues after removal of the skeletal bone, and skin. Briefly, soft tissues were isolated from 3 mice (both legs pooled as one replicate) minced with scissors, and then subject to 0.2% collagenase type II digestion at 37 C for 45 minutes. The digestion was stopped by adding an equal volume of DMEM containing 10% FBS and cells collected by centrifugation at 400 X g for 5 minutes. Debris was removed by filtering with a 70 micron filter. For isolation of cells from peripheral blood, whole blood was layered onto Ficoll-Paque™ Plus (GE Healthcare) and spun according to manufacturer's instructions. The mononuclear cell band was removed, washed with PBS and then immunostained as follows. The cells were next incubated with Claudin 5 antibody (Novus Biological, 1:200 dilution) and/or PDGFR α (Santa Cruz) for 45 minutes on ice. Cells were washed with 1X phosphate buffered saline (PBS) and then incubated with anti-goat Alexa Fluor 488 (Invitrogen, 1:500 dilution) for 30 minutes on ice. Cells were again washed with 1X PBS and stained cells were analyzed on a FACSAria II (BD, Becton Dickson) flow cytometer and BD FACSDiva Software. For cell sorting, labeled cells were separated based on their fluorescence intensity and the Claudin 5 negative and positive population were collected with >95% purity. The percentage of positive cells from each experiment was averaged, the standard error of the mean calculated, and statistical significance was determined by ANOVA with Bonferroni-Holm post-hoc correction for multiple comparisons.

Q-RT-PCR (Real Time PCR) From the harvested muscle tissue surrounding the injection site of either control or BMP2 transduced cells, total RNA was collected using a Trizol reagent (Life Technologies, Carlsbad, CA). RNA integrity was confirmed by agarose gel electrophoresis. cDNA was synthesized from RNA using the RT2 first strand kit (SA Biosciences Inc., Frederick, MD). The cDNA from each sample was analyzed separately, the results were averaged and standard error of the mean calculated. The cDNA from muscles with control or BMP2 transduced cells were subjected to qRT-PCR analysis in parallel using a 7900HT PRISM Real-Time PCR machine (Applied Biosystems, Carlsbad, CA). The C_t values were normalized to both internal 18S ribosomal RNA used in multiplexing and to each other to remove changes in gene expression common to both the control and BMP-2 tissues by using the method of $\Delta\Delta C_t$ along with SYBR Green probes and qPCR primers (SABiosciences, Frederick, MD). The analyses were conducted in triplicate for 8 biological samples at each time point and were reported as the average and standard deviation of the fraction of RNA that was attributed to target cDNA. Significance was determined by ANOVA with Bonferroni-Holm post-hoc correction for multiple comparisons.

Results

BMP2 induces the appearance of osterix in p75⁺ cells in the endoneurium of peripheral nerves: Previous studies (3) suggested that cells present in the endoneurial compartment of peripheral nerves express the osteogenic factor osterix after delivery of AdBMP2-transduced cells.. Therefore tissues were isolated and immunostained on days 1, 2, 4, and 7 after induction of HO through delivery of AdBMP2-transduced cells. Surprisingly, there was significant osterix expression on cells in the endoneurium at 24 h, but this rapidly disappeared within 24 hours as seen on tissues isolated 2 days after induction of HO (Figure 1A). Note in Figure 1A two different primary antibodies represented by two different secondary antibodies were used to confirm this phenomenon and patterns of osterix expression appeared to be similar, independent of the antibody. To confirm the nerve structure, tissues were also immunostained for neurofilament H chain (NF). Two cell types are common within the endoneurial compartment of peripheral nerves, specialized vascular endothelial cells and Schwann cells necessary for myelination of axons. Claudin 5 has previously been shown to be a marker for the specialized endoneurial endothelial cells (8, 31). Therefore, tissues were co-stained for osterix and claudin 5 (Figure 1). As expected, claudin 5 appeared to be associated with vessels and the expression pattern matching CD31⁺ vasculature is shown on a serial section (Figure 1A). Interestingly, the majority of the claudin 5⁺ cells did not appear to co-align with osterix. However by the second day after induction, some of the vessels within the endoneurium express both claudin 5 and CD31, although it is not clear whether osteoprogenitors in these vessels co-express these proteins. Examination of tissues isolated 4 and 7 days after BMP2 induction (Figure 1B) shows co-expression of osterix and claudin 5 in many cells throughout the muscle. Additionally, substantial vessel networks, as assessed by CD31 staining (red, Figure 1B), were observed in the region where the claudin 5⁺ osterix⁺ cells were localized, and these regions were found by day 7 to be associated with bone matrix (Figure 1B, yellow arrows). The data suggests that osteoprogenitors outside the nerve express claudin 5, however the osterix⁺ cells in the endoneurium 24 hours after delivery of BMP2 do not appear to express claudin 5.

We next immunostained cells for the presence of two Schwann cell markers, low-affinity nerve growth factor receptor (p75 (NTR) and myelin protein zero (MPZ) (Figure 1C). It has been previously demonstrated that Schwann cells express elevated levels of p75 (NTR) during peripheral nerve regeneration and myelination (33). However, it has also been shown that neural crest stem cells express p75 (NTR) (34). To distinguish

Schwann cells from neural progenitors, tissues isolated 2 and 6 days after induction of HO were co-immunostained with osterix and either p75 (NTR) or myelin protein zero (MPZ). The results show the co-expression of osterix and p75 within the endoneurium (Figure 1C). MPZ⁺ cells were also observed in this region of the nerve; however these cells did not express osterix (Figure 1C). The results suggest that the osterix⁺ cell within in the endoneurium is either a Schwann cell that is not myelinating or a neural progenitor that resides in the endoneurium of adult nerves as previously described by Morrison et al , 1999 (34).

Claudin 5⁺ osteoprogenitors enter the general circulation shortly after BMP2 induction: Osterix expression was present on the endoneurial cells for only 24 hours after which time we did not observe expression in the nerve (Figure 1A). This suggests that either expression is down regulated or that these cells immediately exit the nerve. One of the only ways for cells to exit the endoneurium of the nerve is through the highly regulated blood-nerve barrier formed by tight and adheren junctions between endoneurial endothelial cells lining the endoneurial vessels. Since claudin 5 is not only an important tight junction protein, but also has been found in blood after barrier disruption (35), mononuclear cells from blood were isolated and tested for the presence of claudin 5⁺ cells at various times after BMP2 induction. The results show that approximately 1 percent of the cells were positive for claudin 5 one day after induction of bone formation, and this was not significantly different from the control. Interestingly, the percentage of claudin 5⁺ cells increased dramatically two days after the induction, with approximately 4.5% of the cells now positive for this marker. However, the increase in cells expressing claudin 5 in blood was short-lived and levels returned to background four days after BMP2 induction (Figure 2A).

To confirm that these circulating claudin 5⁺ cells were expressing osterix, both positive and negative populations were isolated by FACS followed by cytopspin and immunostaining for osterix. All of the osterix expression was found to be in the claudin 5⁺ cells (Figure 2B). The data collectively suggests that cells in the endoneurium that express osterix rapidly exit the nerve through vascular tight junctions that are regulated in part by claudin 5. Upon entering the endoneurial vessels it appears that osteoprogenitors begin to express claudin 5, although the reason for such expression is unclear.

Osteoprogenitors extravasate across the vessel wall when they reach the area of bone formation:

To determine if the process of extravasation (36) is involved in the migration of the claudin 5⁺ osterix⁺ cells through the vessel wall and to the site of bone formation, RNA was isolated from muscle at daily intervals for seven days after BMP2 induction and the levels of RNA specific for known extravasation factors (CXCR4, CD44, SDF, and P and E-selectin) were quantified through qRT-PCR (Figure 3A). The results show a significant increase in CXCR4, CD44 and E-selectin RNAs starting 4 days after induction of HO that was maintained for the remainder of bone formation (Figure 3A), whereas SDF and P-Selectin did not show a significant change (data not shown). As confirmation, claudin 5⁺ and ⁻ cells were isolated from the tissues, spun onto slides that were then immunostained for a factor present on the endothelial cells (E-selectin) as well as factors present on the extravasating cell (CD44 and CXCR4) As expected, the claudin 5⁺ population expressed CD44 and CXCR4 whereas the negative population expressed E-selectin (Figure 3B), suggesting that extravasation through the vessel wall is responsible for the engraftment of the cells at the site of bone formation.

Claudin 5⁺ cells express osteogenic markers after BMP2 induction: Claudin 5⁺ and ⁻ populations of cells were isolated from the tissues surrounding the site of new bone formation four days after BMP2 induction (Figure 4). Cells were immunostained for the osteogenic factors osterix and *dlx 5*. Surprisingly, the majority (90%) of the claudin 5-positive population also stained positively for osterix (Figure 4, panels A-C). Although there were numerous cells in the claudin 5⁻ population, as determined by DAPI staining (panel F), there were virtually no cells staining positively for osterix (Figure 4 panel E). We next performed immunostaining to detect the expression of *dlx5* on the claudin 5⁺ and ⁻ cell populations. *Dlx5* is an osteogenic factor that is expressed during development in the perichondrial region of both the embryonic axial and appendicular skeleton (33) and is thought to be upstream of osterix. It is activated by BMP2 and upregulates both osterix (34) and osteocalcin (30) expression during osteogenesis. *Dlx 5* was expressed only in the claudin 5⁺ cell population, although some of the cells were not positive for this factor (Figure 4, panels G-I) the claudin 5⁻ population was completely negative for *dlx5* expression (Figure 4, panel K).

Claudin 5⁺ cells express factors associated with nerve stem/progenitor cells: Claudin 5⁺ cells were further characterized for the expression of two additional nerve stem/progenitor cell markers, PDGFR α and musashi. Both PDGFR α , a factor associated with perivascular astrocytes (21) and shown to be involved in glial-endothelial cell interactions and critical for maintenance of the blood-brain barrier (21), and musashi, which is an RNA binding protein that is highly specific for neural stem cells (37) and is not expressed in fully differentiated cells (38) (39), were assessed on the claudin 5⁺ cells. FACS analysis showed that PDGFR α was expressed on these cells (Figure 5A). Analysis of the cells showed the absence of a claudin 5⁺ PDGFR α ⁻ population although we did observe a small PDGFR α ⁺ claudin 5⁻ population (Figure 5A) that may represent Schwann cells, which previously have been shown to be positive for this receptor (40).

Again claudin 5⁺ and ⁻ populations isolated from tissues two days after delivery of the AdBMP2-transduced cells were isolated and immunostained for musashi. Almost all the cells in the claudin 5⁺ population were also musashi⁺ (Figure 5B, panels G-I). Positive immunostaining for musashi was not observed in the claudin 5⁻ population although there were an equal number of cells on the slides (Figure 5B, panels J-L). Overall the data suggests that these osteoprogenitor cells, in addition to the upregulation of osteogenic factors, also express neural crest markers, which may be remnants of their neural origin.

Claudin 5⁺ cells express the endothelial marker Tie-2: Since others have reported the presence of PDGFR α on the surface of an osteoprogenitor expressing Tie 2, the claudin 5⁺ and ⁻ populations were immunostained for Tie-2 (Figure 6A). Almost all of the claudin 5⁺ cells were found to express Tie-2, but there appeared to be a wide variation in its expression level (Figure 6A). Additionally, we noted that in some cases Tie 2 had a surprisingly asymmetric localization on cells (Figure 6B), which may indicate a migrating, rather than matrix bound, cell as described by Saharinen *et al* (41). The data collectively suggest that these osteoprogenitors express not only osteogenic transcription factors (osterix and dlx 5), but also markers of early neural (mushasi and PDGF α), and vascular (Tie-2) progenitors. Hence the progenitors, although bound for a potentially unique destination (bone), are expressing a variety of markers that may allow them to be recruited for a variety of fates.

Discussion

The results show the presence of osterix⁺ cells in the endoneurium of peripheral nerves immediately after HO induction through delivery of AdBMP2 transduced cells. These cells then disappear at the same time as the appearance of osterix⁺ claudin 5⁺ cells in the circulation. Within four days after induction of HO they disappear from the blood stream simultaneously with an increase in expression of factors involved in cell extravasation and the appearance of the osterix⁺ claudin 5⁺ cells in muscle at the site of heterotopic ossification. The data suggests that these osteoprogenitors exit the nerve through the blood-nerve barrier, enter the circulation, and home to the site of HO.

The reason for expression of claudin 5 by these osteoprogenitors is not clear. It has been shown that cells expressing claudin 5 have not only increased adherence, but also increased motility (42) consistent with the ability of these osteoprogenitors to circulate. Interestingly, endothelial progenitors have previously been shown to leave the vessel wall and circulate (43) suggesting that the osterix⁺ claudin 5⁺ p75⁺ cells may function similarly to these endothelial progenitors.

These osterix⁺ claudin 5⁺ p75⁺ cells then appear to home to the site of bone formation. We previously showed the rapid expansion of new vessels after delivery of the AdBMP2- transduced cells (44) and in the current study an extensive vascular plexus can be seen surrounding the claudin 5⁺ osterix⁺ cells. Further, at this same time, extravasation factors (CXCR4, CD44, and E-selectin) were significantly elevated in these tissues consistent with the appearance, through the circulation, of the cells at this site. It has been previously shown that CD44 is a key mediator of the transendothelial migration of many cell types and mediates the binding of CD44 to hyaluronic acid on the endothelial cell (45) (36, 46). Further, invasion of calcified cartilage by vessels is a key event in endochondral bone formation (47). Therefore, CD44 which is expressed on the surface of the osteoprogenitor likely binds to the E-selectin on the surface of the endothelial cells. This is the first step of extravasation. Additionally the cells appear to express CXCR4, which is also significantly elevated in the tissues at this time; CXCR4 has been shown to bind SDF 1 on endothelial cells, as the second step in extravasation, which allows for tighter binding, and eventually migration through pores between the endothelial cells (48). SDF 1 RNA within the tissues did not change significantly during HO; however, it was present in the tissues (data not shown). Additionally the new vessels that are rapidly forming at this site are tiny with the

significant branches, suggesting lower flow, necessary for depositing cells. Finally new vessels or venules must undergo remodeling to organize the structure and support greater blood flow without leaking (49). Thus it is highly likely at this stage for cells to traverse the vessel wall more easily than in mature vessels.

Phenotypic characterization of these cells shows expression of Tie-2, a marker of endothelial cells. The presence of endothelial markers on osteoprogenitors has also recently been described by others (50) (13). Additionally these cells express musashi and p75 that are phenotypic markers of neural crest stem cells (37) (34, 38, 39). In addition to these neural crest markers, the cells also express PDGFR α , a factor involved in glial-endothelial cell interactions and critical for maintenance of the blood-brain barrier, suggesting that endothelial-neural cell interaction may play a key role in transition of these progenitors from a neural to mesodermal fate.

It is possible that BMP2 induction of bone formation in the adult is, at least in part, a re-capitulation of embryonic bone formation. The formation of craniofacial bone and cartilage in the embryo begins with neural crest stem cell migration from the neural tube (51). One of the key factors that indicate the start of osteogenesis in these cells is the expression of dlx5 and osterix, similar to the early osteogenic factors on the osterix⁺ claudin 5⁺ p75⁺progenitors.. The synthesis of osteoblasts from neural crest stem cells uses a combination of Wnt and BMP signaling. Although Wnt 1 is the major inducer of neural crest (52), when it is unopposed Wnt 1 signaling leads to the production of sensory nerves from neural stem cells (53). However, when opposed by BMP2, Wnt 1 signaling in neural crest stem cells leads to other cell types including osteoprogenitors (54). Thus the biogenesis of osteoprogenitors in the adult may ultimately originate from neural stem cells housed in the endoneurium. It is conceivable that these cells may have been deposited within the endoneurium during neural crest migration and formation of sensory nerves. Perhaps neural crest stem cells are deposited in all neural crest tissues, since several reports suggest a Wnt1⁺ neural crest stem cell in the jaw. Alternatively, these cells may simply persist in the endoneurium because it is an immune privileged location. Therefore, they were never exposed to and cleared by the adult immune system. Such a mechanism would also allow tissue regeneration using a recapitulation of an embryonic process.

The current study also underscores the importance of barriers or interfaces between blood and nerves in heterotopic ossification. Two molecules that show dramatic increase upon BMP2 induction of heterotopic ossification, claudin 5 and PDGFR α are either a key component or regulator, respectively, of these barriers.

Recently it has become very obvious that there is a relationship between traumatic brain injury and HO (55). One possible reason that HO is associated with traumatic brain injury, which causes a breakdown in the blood-brain barrier (55, 56) could be that changes in this barrier, leads to the exit of these neural progenitors that can engraft and become osteoblasts, particularly at sites where BMP2 may be present such as those that have also sustained a fracture.

The data collectively suggests that neural progenitors within the endoneurium of peripheral nerves can undergo osteogenic differentiation, and migrate from the nerve, through the circulation to the site of new bone formation. Many recent studies suggest that osteoprogenitors are local progenitors, either recruited from vasculature or from interstitial spaces between muscle fibers (13) (14). Our data actually supports not only a circulating progenitor, but also a local progenitor, because the cells engraft several days prior to the appearance of cartilage or bone. Therefore these fibroblast-like cells deposited between the muscle fibers, would appear to be local cells. Further, if this is a recapitulation of neural crest formation of the bones and cartilage of the head, then presumably this is not endochondral bone formation but rather two independent processes. Thus, it may not be surprising that these osteogenic cells appear in a location distinct from the cartilage and arrive prior to its formation. In conclusion, these studies are the first to demonstrate the presence of a progenitor within peripheral nerves that responds to BMP2 by undergoing both osteogenic differentiation and homing to the location of bone formation.

Disclosures

All authors state that they have no conflicts of interest.

Acknowledgements

This work was supported by grants from the DOD (DAMD W81XWH-12-1-0274, "Diagnosis and Treatment of Heterotopic Ossification) and NIH-NIAMS (R21AR061638, "Heterotopic Bone from Stem Cells in Nerve; R21AR063779 Function of Brown Adipose in Bone Formation; R01AR066556, Neural Mechanisms in Heterotopic Ossification) , EAS was supported by a postdoctoral fellowship (NIH NIGMS K12 GM084897).

.Authors' roles: ZWL, EAO, EB, EAS, and RPN contributed to design, data acquisition, analysis, and interpretation. EAO, EHU, ZG and ARD contributed to data acquisition, analysis, and interpretation. EAO,

EHU, ZG, and ARD contributed to design and interpretation. EAO and ARD drafted the initial manuscript and the remaining authors critically revised the manuscript. All authors approved the final version of the manuscript.

References

1. Salisbury EA, Lazard ZW, Ubogu EE, Davis AR, Olmsted-Davis EA 2012 Transient brown adipocyte-like cells derive from peripheral nerve progenitors in response to bone morphogenetic protein 2. *Stem Cells Transl Med* **1**(12):874-85.
2. Pittenger MF, Mackay AM, Beck SC, Jaiswal RK, Douglas R, Mosca JD, Moorman MA, Simonetti DW, Craig S, Marshak DR 1999 Multilineage potential of adult human mesenchymal stem cells. *Science* **284**(5411):143-7.
3. Suda RK, Billings PC, Egan KP, Kim JH, McCarrick-Walmsley R, Glaser DL, Porter DL, Shore EM, Pignolo RJ 2009 Circulating osteogenic precursor cells in heterotopic bone formation. *Stem Cells* **27**(9):2209-19.
4. Kumagai K, Vasanji A, Drazba JA, Butler RS, Muschler GF 2008 Circulating cells with osteogenic potential are physiologically mobilized into the fracture healing site in the parabiotic mice model. *J Orthop Res* **26**(2):165-75.
5. Otsuru S, Tamai K, Yamazaki T, Yoshikawa H, Kaneda Y 2008 Circulating bone marrow-derived osteoblast progenitor cells are recruited to the bone-forming site by the CXCR4/stromal cell-derived factor-1 pathway. *Stem Cells* **26**(1):223-34.
6. Medici D, Shore EM, Lounev VY, Kaplan FS, Kalluri R, Olsen BR 2010 Conversion of vascular endothelial cells into multipotent stem-like cells. *Nat Med* **16**(12):1400-6.
7. Lounev VY, Ramachandran R, Wosczyzna MN, Yamamoto M, Maidment AD, Shore EM, Glaser DL, Goldhamer DJ, Kaplan FS 2009 Identification of progenitor cells that contribute to heterotopic skeletogenesis. *J Bone Joint Surg Am* **91**(3):652-63.
8. Salisbury E, Rodenberg E, Sonnet C, Hipp J, Gannon FH, Vadakkan TJ, Dickinson ME, Olmsted-Davis EA, Davis AR 2011 Sensory nerve induced inflammation contributes to heterotopic ossification. *J Cell Biochem* **112**(10):2748-58.
9. Wosczyzna MN, Biswas AA, Cogswell CA, Goldhamer DJ 2012 Multipotent progenitors resident in the skeletal muscle interstitium exhibit robust BMP-dependent osteogenic activity and mediate heterotopic ossification. *J Bone Miner Res* **27**(5):1004-17.
10. Cairns DM, Liu R, Sen M, Canner JP, Schindeler A, Little DG, Zeng L 2012 Interplay of Nkx3.2, Sox9 and Pax3 regulates chondrogenic differentiation of muscle progenitor cells. *PLoS One* **7**(7):e39642.
11. Jackson WM, Aragon AB, Bulken-Hoover JD, Nesti LJ, Tuan RS 2009 Putative heterotopic ossification progenitor cells derived from traumatized muscle. *J Orthop Res* **27**(12):1645-51.
12. Polfer EM, Forsberg JA, Fleming ME, Potter BK 2013 Neurovascular entrapment due to combat-related heterotopic ossification in the lower extremity. *J Bone Joint Surg Am* **95**(24):e195(1-6).
13. Pringle N, Collarini EJ, Mosley MJ, Heldin CH, Westermark B, Richardson WD 1989 PDGF A chain homodimers drive proliferation of bipotential (O-2A) glial progenitor cells in the developing rat optic nerve. *EMBO J* **8**(4):1049-56.
14. Richardson WD, Pringle N, Mosley MJ, Westermark B, Dubois-Dalcq M 1988 A role for platelet-derived growth factor in normal gliogenesis in the central nervous system. *Cell* **53**(2):309-19.

15. Su EJ, Fredriksson L, Geyer M, Folestad E, Cale J, Andrae J, Gao Y, Pietras K, Mann K, Yepes M, Strickland DK, Betsholtz C, Eriksson U, Lawrence DA 2008 Activation of PDGF-CC by tissue plasminogen activator impairs blood-brain barrier integrity during ischemic stroke. *Nat Med* **14**(7):731-7.
16. Olmsted-Davis EA, Gugala Z, Gannon FH, Yotnda P, McAlhany RE, Lindsey RW, Davis AR 2002 Use of a chimeric adenovirus vector enhances BMP2 production and bone formation. *Hum Gene Ther* **13**(11):1337-47.
17. Gugala Z, Olmsted-Davis EA, Gannon FH, Lindsey RW, Davis AR 2003 Osteoinduction by ex vivo adenovirus-mediated BMP2 delivery is independent of cell type. *Gene Ther* **10**(16):1289-96.
18. Fouletier-Dilling CM, Bosch P, Davis AR, Shafer JA, Stice SL, Gugala Z, Gannon FH, Olmsted-Davis EA 2005 Novel compound enables high-level adenovirus transduction in the absence of an adenovirus-specific receptor. *Hum Gene Ther* **16**(11):1287-97.
19. Fouletier-Dilling CM, Gannon FH, Olmsted-Davis EA, Lazard Z, Heggeness MH, Shafer JA, Hipp JA, Davis AR 2007 Efficient and rapid osteoinduction in an immune-competent host. *Hum Gene Ther* **18**(8):733-45.
20. Olmsted-Davis E, Gannon FH, Ozen M, Ittmann MM, Gugala Z, Hipp JA, Moran KM, Fouletier-Dilling CM, Schumara-Martin S, Lindsey RW, Heggeness MH, Brenner MK, Davis AR 2007 Hypoxic adipocytes pattern early heterotopic bone formation. *Am J Pathol* **170**(2):620-32.
21. Kan L, Lounev VY, Pignolo RJ, Duan L, Liu Y, Stock SR, McGuire TL, Lu B, Gerard NP, Shore EM, Kaplan FS, Kessler JA 2011 Substance P signaling mediates BMP-dependent heterotopic ossification. *J Cell Biochem* **112**(10):2759-72.
22. Nakashima K, Zhou X, Kunkel G, Zhang Z, Deng JM, Behringer RR, de Crombrughe B 2002 The novel zinc finger-containing transcription factor osterix is required for osteoblast differentiation and bone formation. *Cell* **108**(1):17-29.
23. Mizisin AP, Weerasuriya A 2011 Homeostatic regulation of the endoneurial microenvironment during development, aging and in response to trauma, disease and toxic insult. *Acta Neuropathol* **121**(3):291-312.
24. Weerasuriya A, Mizisin AP 2011 The blood-nerve barrier: structure and functional significance. *Methods Mol Biol* **686**:149-73.
25. Yosef N, Ubogu EE 2013 An immortalized human blood-nerve barrier endothelial cell line for in vitro permeability studies. *Cell Mol Neurobiol* **33**(2):175-86.
26. Yosef N, Xia RH, Ubogu EE 2010 Development and characterization of a novel human in vitro blood-nerve barrier model using primary endoneurial endothelial cells. *J Neuropathol Exp Neurol* **69**(1):82-97.
27. Ubogu EE 2013 The molecular and biophysical characterization of the human blood-nerve barrier: current concepts. *J Vasc Res* **50**(4):289-303.
28. Nitta T, Hata M, Gotoh S, Seo Y, Sasaki H, Hashimoto N, Furuse M, Tsukita S 2003 Size-selective loosening of the blood-brain barrier in claudin-5-deficient mice. *J Cell Biol* **161**(3):653-60.
29. Cosgaya JM, Chan JR, Shooter EM 2002 The neurotrophin receptor p75NTR as a positive modulator of myelination. *Science* **298**(5596):1245-8.
30. Morrison SJ, White PM, Zock C, Anderson DJ 1999 Prospective identification, isolation by flow cytometry, and in vivo self-renewal of multipotent mammalian neural crest stem cells. *Cell* **96**(5):737-49.
31. Kazmierski R, Michalak S, Wencel-Warot A, Nowinski WL 2012 Serum tight-junction proteins predict hemorrhagic transformation in ischemic stroke patients. *Neurology* **79**(16):1677-85.
32. Rampon C, Weiss N, Deboux C, Chaverot N, Miller F, Buchet D, Tricoire-Leignel H, Cazaubon S, Baron-Van Evercooren A, Couraud PO 2008 Molecular mechanism of systemic delivery of neural precursor cells to the brain: assembly of brain endothelial apical cups and control of transmigration by CD44. *Stem Cells* **26**(7):1673-82.

33. Nakamura M, Okano H, Blendy JA, Montell C 1994 Musashi, a neural RNA-binding protein required for Drosophila adult external sensory organ development. *Neuron* **13**(1):67-81.
34. Okano H, Kawahara H, Toriya M, Nakao K, Shibata S, Imai T 2005 Function of RNA-binding protein Musashi-1 in stem cells. *Exp Cell Res* **306**(2):349-56.
35. Battelli C, Nikopoulos GN, Mitchell JG, Verdi JM 2006 The RNA-binding protein Musashi-1 regulates neural development through the translational repression of p21WAF-1. *Mol Cell Neurosci* **31**(1):85-96.
36. Eccleston PA, Funa K, Heldin CH 1993 Expression of platelet-derived growth factor (PDGF) and PDGF alpha- and beta-receptors in the peripheral nervous system: an analysis of sciatic nerve and dorsal root ganglia. *Dev Biol* **155**(2):459-70.
37. Saharinen P, Eklund L, Miettinen J, Wirkkala R, Anisimov A, Winderlich M, Nottebaum A, Vestweber D, Deutsch U, Koh GY, Olsen BR, Alitalo K 2008 Angiopoietins assemble distinct Tie2 signalling complexes in endothelial cell-cell and cell-matrix contacts. *Nat Cell Biol* **10**(5):527-37.
38. Escudero-Esparza A, Jiang WG, Martin TA 2012 Claudin-5 is involved in breast cancer cell motility through the N-WASP and ROCK signalling pathways. *J Exp Clin Cancer Res* **31**:43.
39. Asahara T, Murohara T, Sullivan A, Silver M, van der Zee R, Li T, Witzenbichler B, Schatteman G, Isner JM 1997 Isolation of putative progenitor endothelial cells for angiogenesis. *Science* **275**(5302):964-7.
40. Dilling CF, Wada AM, Lazard ZW, Salisbury EA, Gannon FH, Vadakkan TJ, Gao L, Hirschi K, Dickinson ME, Davis AR, Olmsted-Davis EA 2010 Vessel formation is induced prior to the appearance of cartilage in BMP-2-mediated heterotopic ossification. *J Bone Miner Res* **25**(5):1147-56.
41. DeGrendele HC, Estess P, Picker LJ, Siegelman MH 1996 CD44 and its ligand hyaluronate mediate rolling under physiologic flow: a novel lymphocyte-endothelial cell primary adhesion pathway. *J Exp Med* **183**(3):1119-30.
42. DeGrendele HC, Estess P, Siegelman MH 1997 Requirement for CD44 in activated T cell extravasation into an inflammatory site. *Science* **278**(5338):672-5.
43. Gerber HP, Vu TH, Ryan AM, Kowalski J, Werb Z, Ferrara N 1999 VEGF couples hypertrophic cartilage remodeling, ossification and angiogenesis during endochondral bone formation. *Nat Med* **5**(6):623-8.
44. Oberlin E, Amara A, Bachelier F, Bessia C, Virelizier JL, Arenzana-Seisdedos F, Schwartz O, Heard JM, Clark-Lewis I, Legler DF, Loetscher M, Baggiolini M, Moser B 1996 The CXC chemokine SDF-1 is the ligand for LESTR/fusin and prevents infection by T-cell-line-adapted HIV-1. *Nature* **382**(6594):833-5.
45. Wagner DD, Frenette PS 2008 The vessel wall and its interactions. *Blood* **111**(11):5271-81.
46. Decker B, Bartels H, Decker S 1995 Relationships between endothelial cells, pericytes, and osteoblasts during bone formation in the sheep femur following implantation of tricalciumphosphate-ceramic. *Anat Rec* **242**(3):310-20.
47. Mishina Y, Snider TN 2014 Neural crest cell signaling pathways critical to cranial bone development and pathology. *Exp Cell Res*.
48. Garcia-Castro MI, Marcelle C, Bronner-Fraser M 2002 Ectodermal Wnt function as a neural crest inducer. *Science* **297**(5582):848-51.
49. Lee HY, Kleber M, Hari L, Brault V, Suter U, Taketo MM, Kemler R, Sommer L 2004 Instructive role of Wnt/beta-catenin in sensory fate specification in neural crest stem cells. *Science* **303**(5660):1020-3.
50. Kleber M, Lee HY, Wurdak H, Buchstaller J, Riccomagno MM, Ittner LM, Suter U, Epstein DJ, Sommer L 2005 Neural crest stem cell maintenance by combinatorial Wnt and BMP signaling. *J Cell Biol* **169**(2):309-20.
51. Sullivan MP, Torres SJ, Mehta S, Ahn J 2013 Heterotopic ossification after central nervous system trauma: A current review. *Bone Joint Res* **2**(3):51-7.

52. Shlosberg D, Benifla M, Kaufer D, Friedman A 2010 Blood-brain barrier breakdown as a therapeutic target in traumatic brain injury. *Nat Rev Neurol* **6**(7):393-403.

Legends to Figures

Figure 1A. Osterix expression begins in the endoneurium of peripheral nerves. C57BL/6 mice (n=8) were injected with BMP2 producing cells 4 mice were euthanized at day 1 and 2. Frozen sections were prepared and immunostained for Neurofilament heavy chain (NF), CD31, or osterix. Colors are as indicated. DAPI is blue. H and E, sections were stained with hematoxylin and eosin.

Figure 1B. Expression of osterix, claudin 5, and CD31 at later times after BMP2 induction. C57BL/6 mice (n=16) were injected with BMP2 producing cells and 8 mice were euthanized at either day 4 or 7. Frozen sections were prepared and immunostained for CD31, claudin 5, or osterix as indicated. DAPI is blue.

Figure 1C. Osteoprogenitors for heterotopic ossification are not derived from de-differentiating Schwann cells. Osteoprogenitors in peripheral nerves were assessed at early (one day) and late (six days) after BMP2 induction by analyzing frozen serial sections of C57BL/6 mice (n=4 per group) euthanized 1 and 6 days after BMP2 induction. Sections were analyzed by immunohistochemistry for p75(NTR), osterix, and MPZ. Colors are as indicated.

Figure 2A. Cells expressing claudin 5 increase in blood after BMP2 induction. C57/BL6 mice (n=4 per group) either remained untreated or were injected with BMP2-producing cells. Mice were bled by cardiac puncture at 0 (untreated), 1, 2, and 4 days after induction. Mononuclear cells were collected, reacted with an antibody to claudin 5 and subjected to FACS. Descriptive statistics was used to analyze the study results. The sample size in the groups was n=3. The analysis of variance (ANOVA) with Bonferroni-Holm post-hoc correction for multiple comparisons was used to detect statistically-significant differences between the number of claudin 5⁺ cells present in the circulation at given time points after intramuscular injection of BMP2-producing cells. The thresholds for statistically-significant differences were set at p<0.05.

Figure 2B. Claudin 5⁺ circulating osteoprogenitors express osterix. Cells were isolated from muscle two days after BMP2 induction and claudin 5⁺ and ⁻ cells isolated by preparative FACS. Each population was then subjected to cytopsin and the resultant slides reacted with an antibody to osterix (red). Claudin 5, green; DAPI, blue. Claudin 5 positive population, A, B, and C; Claudin 5 negative population, E, F, and G).

Figure 3A. CD44, CXCR4, and E-selectin are expressed upon BMP2 induction. C57/BL6 mice were injected with BMP2-producing cells (n=8 per group) and at the times indicated mice were euthanized, RNA extracted from muscle around the site of injection, and the relative amount of RNA encoding **A) CD44; B) CXCR4, and C) E-selectin** was determined and comparisons to determine statistically significant differences were made using an analysis of variance (ANOVA) with Bonferroni-Holm post-hoc correction for multiple comparisons. The thresholds for statistically-significant differences were set at p<0.05.

Figure 3B: Claudin 5⁺ cells express CD44 and CXCR4 while claudin 5⁻ cells express E-selectin. C57BL/6 mice (n=4 per group) were injected with BMP2-producing cells and mice were euthanized four days later. Claudin 5⁺ and claudin 5⁻ cells were isolated by preparative FACS, subjected to cytopsin, and the resulting slides analyzed for staining for CD44, E-selectin, and CD44.

Figure 4. Claudin 5-positive cells express osteogenic markers. The claudin 5⁺ population (green) was isolated from a FACS of cells isolated from muscle 4 days after BMP2 induction. These isolated cells were subjected to cytopsin and the slides were then probed with antibodies for claudin 5 (green) and osterix (red). A, B, and C shows one field obtained from the claudin 5⁺ population with C being the merger of A and B; D, E, and F show one field of the cytopsin of a claudin 5⁻ population obtained from the same mouse that was stained with antibodies against claudin 5 (green) and osterix (red) as well as DAPI (F). In the claudin 5⁺ cell population osterix positive cells were found to be 75% ± 3 %. In panels G-I and J-L, respectively, we show the cytopsin patterns of the claudin 5 positive and negative populations of another mouse after staining for claudin 5 (green) and *dlx 5* (red).

Figure 5A. Neural markers expressed in claudin 5 positive cells. C57BL/6 mice were either injected in the quadriceps with BMP2-producing cells or remained uninjected. After 4 days mice were euthanized and cells were isolated from the tissue around the site of injection, reacted with tagged antibodies against claudin 5 and PDGFR α and percentage of the total population positive for both markers was determined by FACS.

Figure 5B. Expression of musashi 1 in claudin 5 positive cells. C57BL/6 mice were either injected in the quadriceps with BMP2-producing cells, A-F or remained uninjected, G-L. After 4 days the mice were euthanized and cells from muscle around the site of injection were isolated, reacted with an antibody against claudin 5 tagged with Alexa fluor 488 (green) and subjected to FACS. The claudin 5 positive (A-C and G-I) and claudin 5 negative (D-F and J-L) populations were isolated from both the BMP2-induced as well as uninjected mice, subjected to cytopspin and the resultant slides stained with DAPI (blue) and an antibody to musashi 1 (red).

Figure 6 A. Osteoprogenitors express the endothelial marker Tie 2. C57/BL6 mice were injected with BMP2-producing cells (n=4) and four days after induction the mice were euthanized and cells harvested from the muscle around the site of injection were separated by FACS into claudin 5 positive and negative populations. The populations were subjected to cytopspin and the slides were assessed for expression of Tie2 (red). Claudin 5, green; DAPI, blue. **B.** This is a representative photomicrograph 40X magnification showing an asymmetric distribution of Tie-2 (red) in some of the cells.

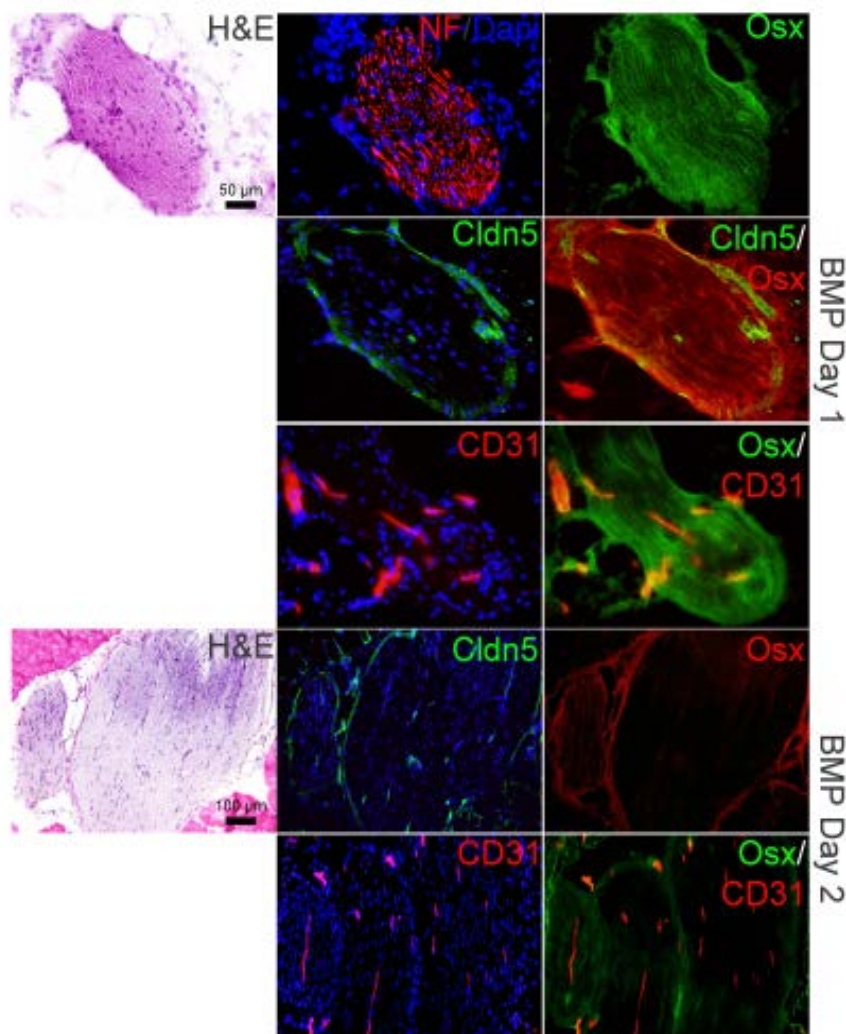


Figure 1A

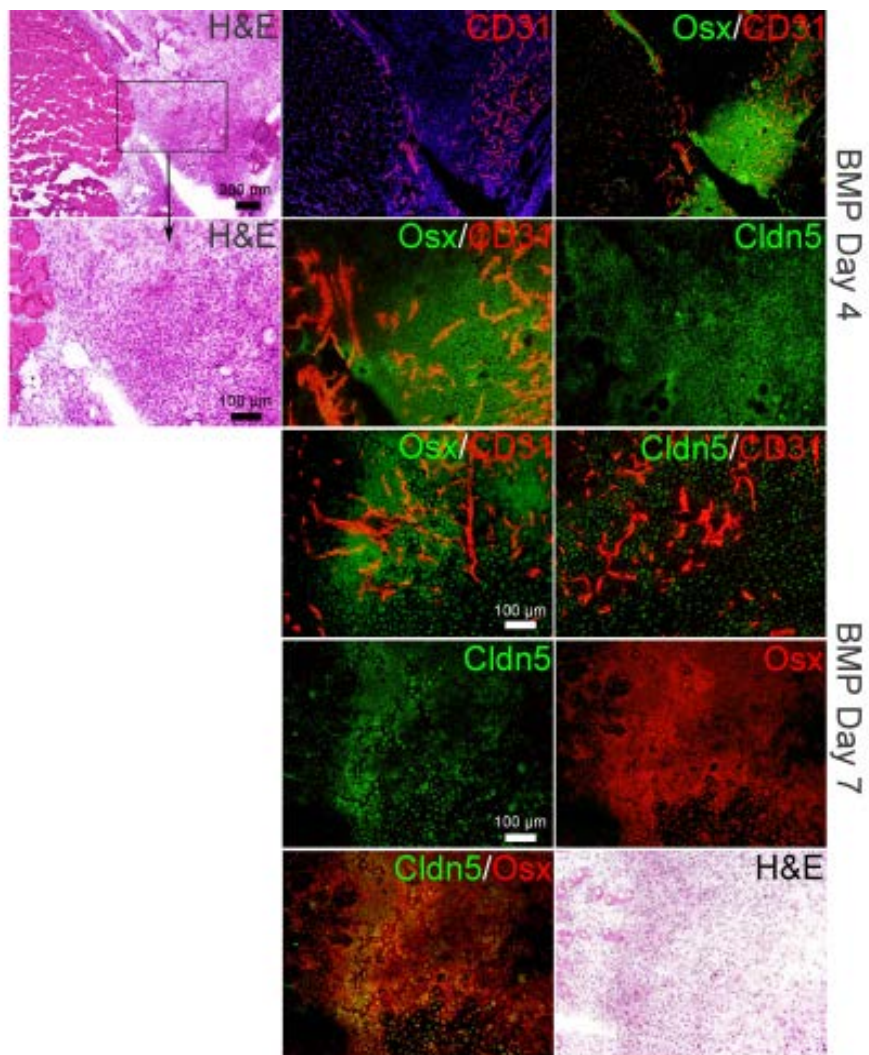


Figure 1B

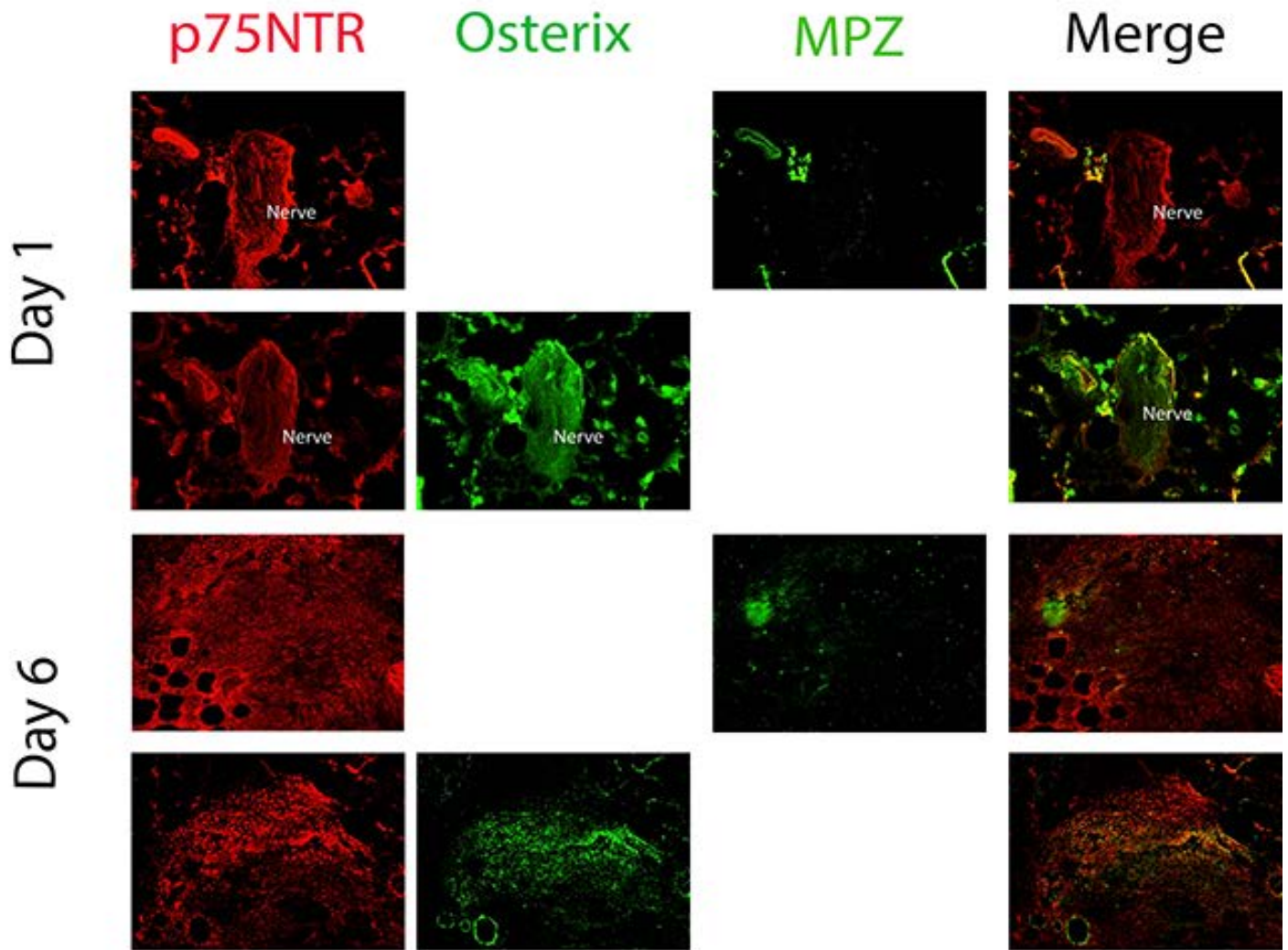


Figure 1C

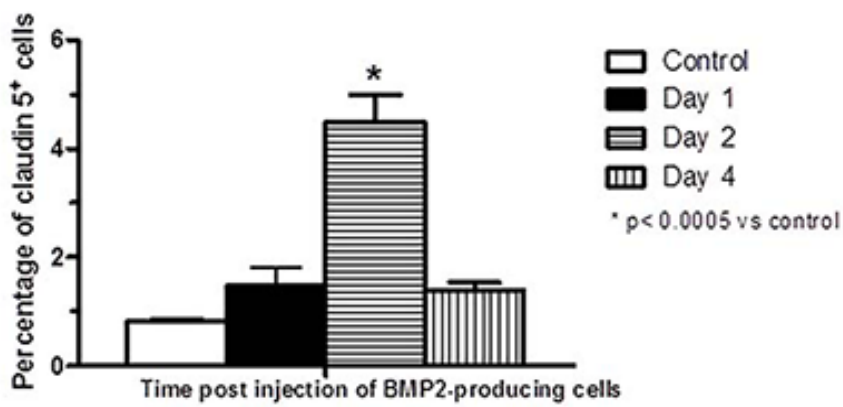


Figure 2A

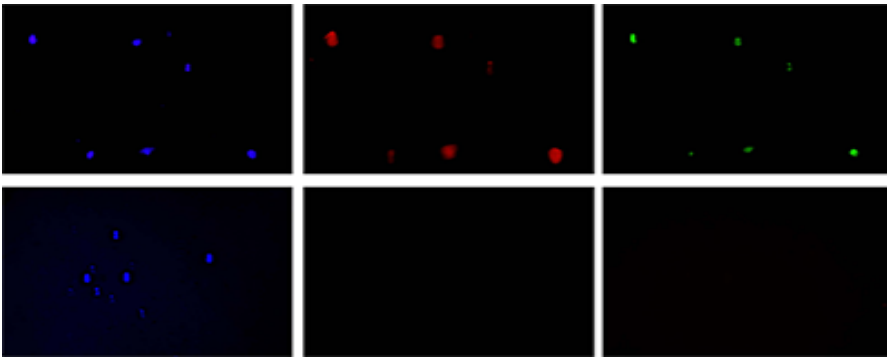


Figure 2B

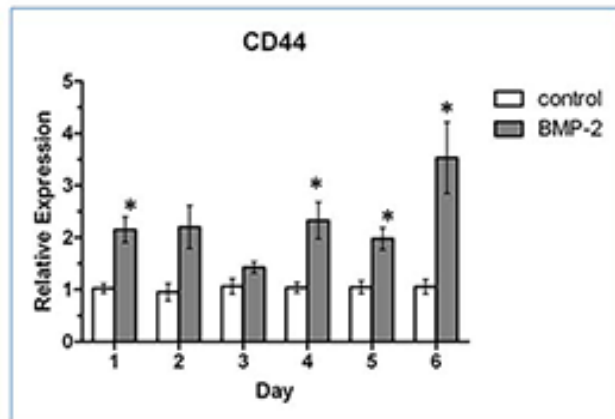
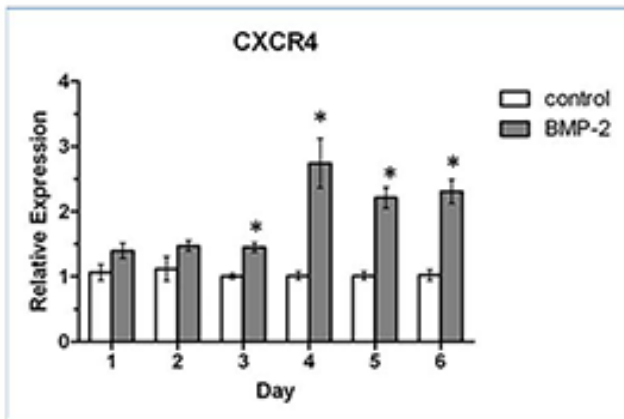
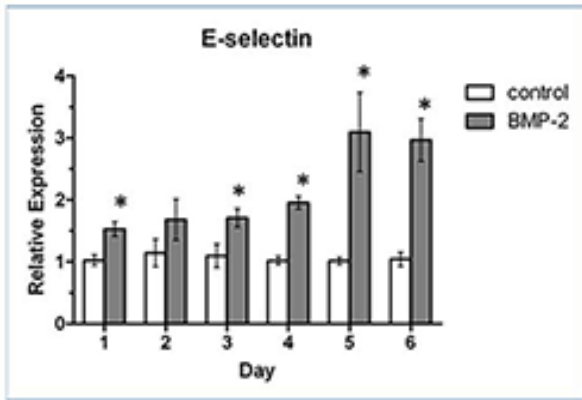


Figure 3A

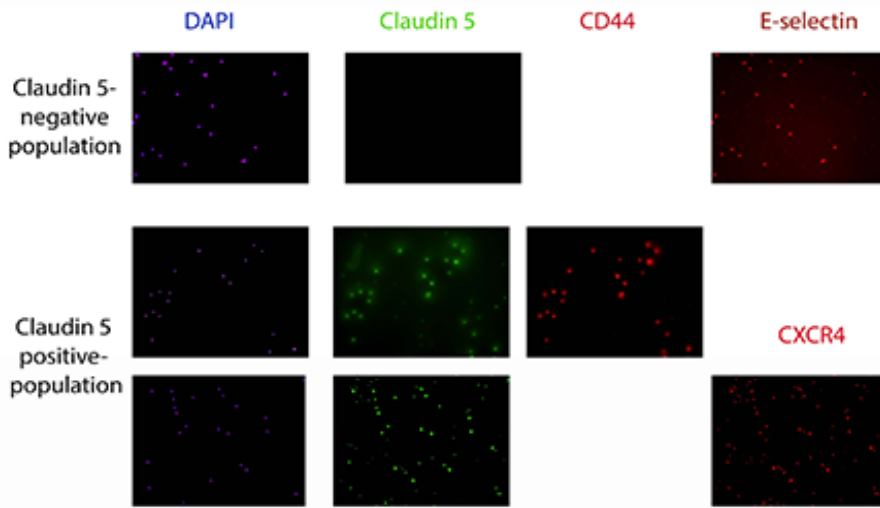


Figure 3B

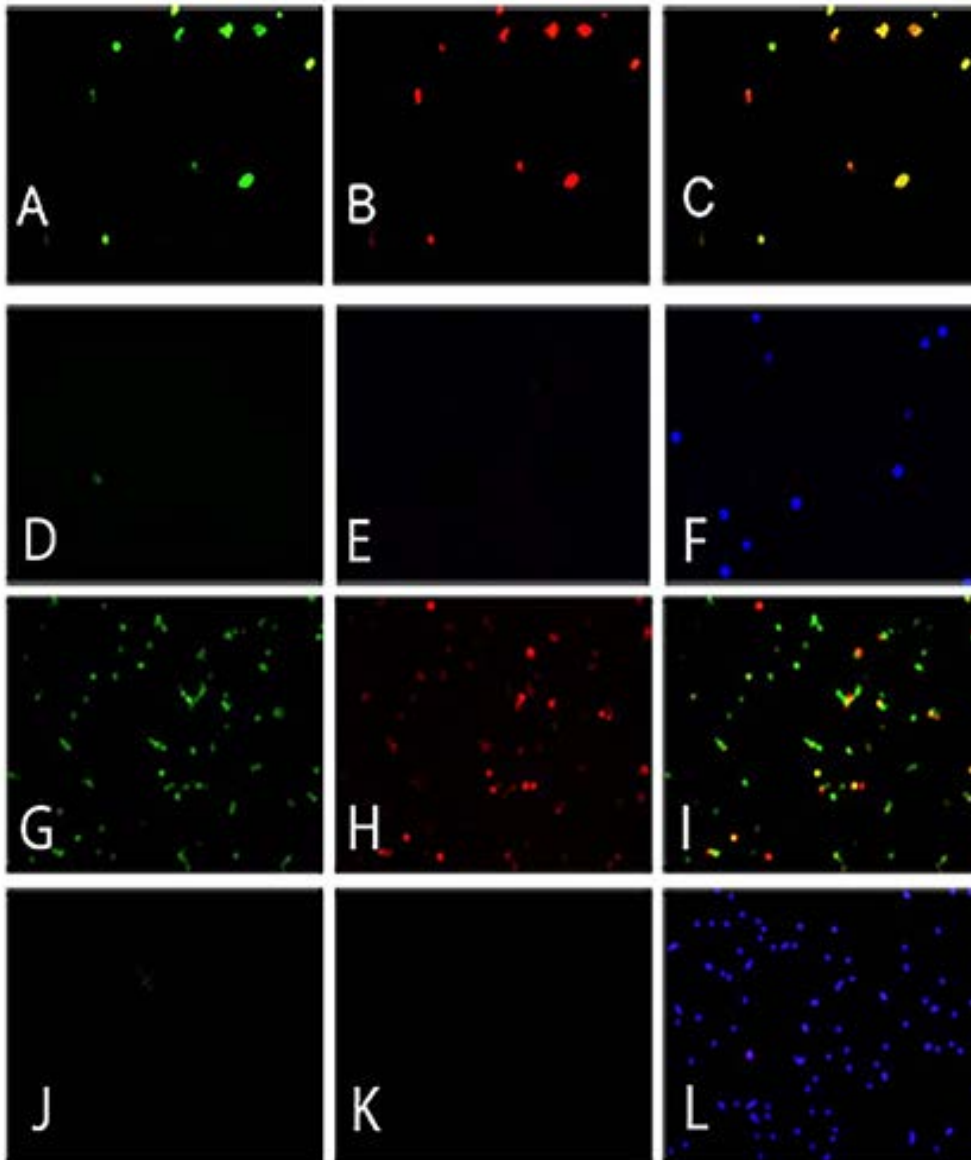


Figure 4

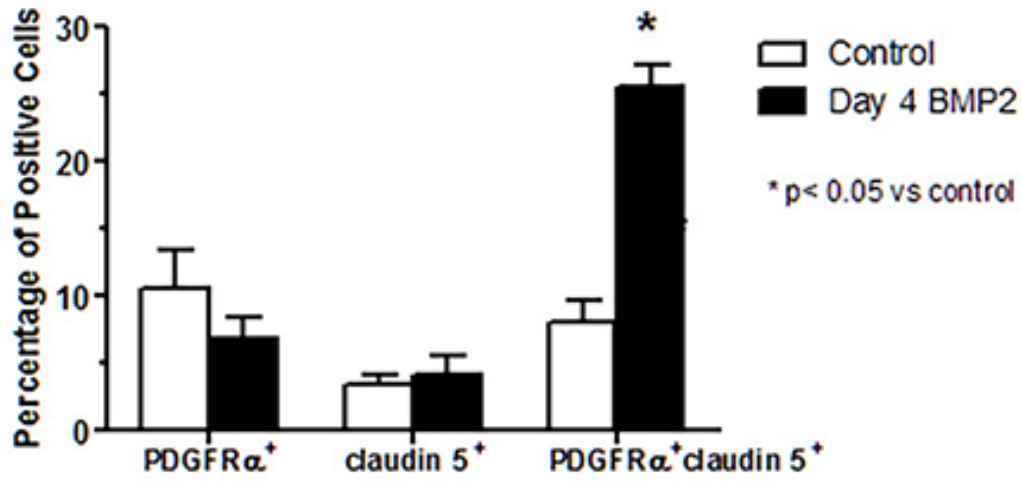


Figure 5A

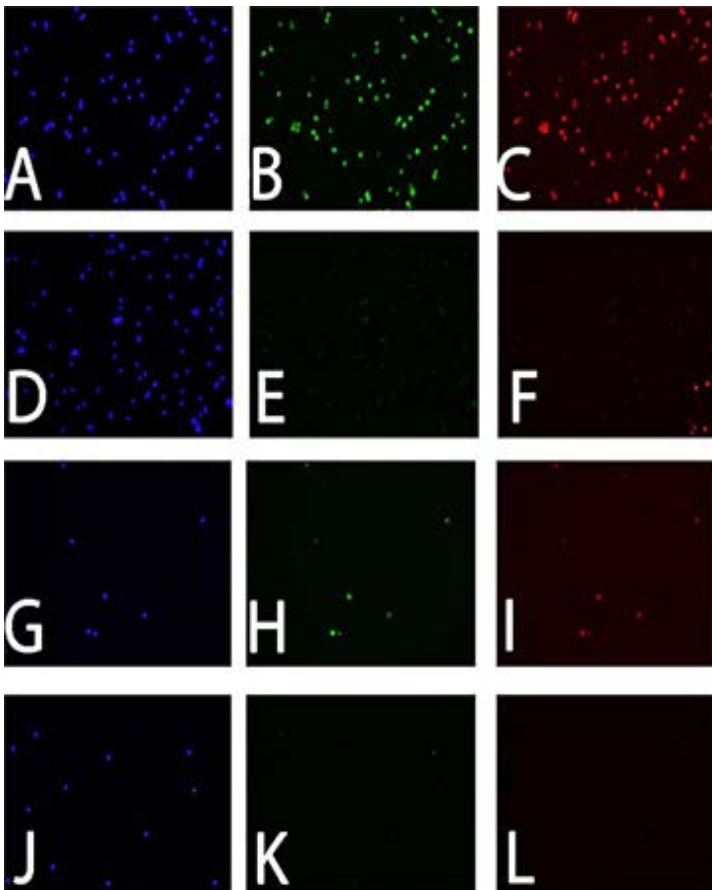
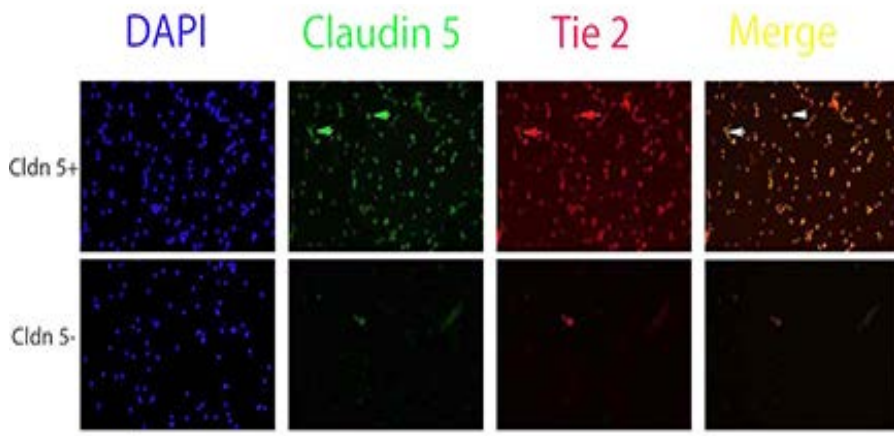


Figure 5B



A



B

Figure 6